

## Ecosystem-scale nutrient cycling responses to increasing air temperatures vary with lake trophic state



Kaitlin J. Farrell<sup>a,b,\*</sup>, Nicole K. Ward<sup>a</sup>, Arianna I. Krinos<sup>a,1</sup>, Paul C. Hanson<sup>c</sup>, Vahid Daneshmand<sup>d</sup>, Renato J. Figueiredo<sup>d</sup>, Cayelan C. Carey<sup>a</sup>

<sup>a</sup> Department of Biological Sciences, Virginia Tech, 926 West Campus Drive, Blacksburg, VA, 24061 USA

<sup>b</sup> Odum School of Ecology, University of Georgia, 140 E. Green Street, Athens, GA, 30602 USA

<sup>c</sup> Center for Limnology, University of Wisconsin-Madison, 680 N. Park Street, Madison, WI, 53706, USA

<sup>d</sup> Advanced Computing and Information Systems Laboratory, University of Florida, 968 Center Drive, Gainesville, FL, 32611, USA

### ARTICLE INFO

#### Keywords:

Biogeochemical cycling  
Climate change  
Distributed computing  
Grapler  
Nutrients  
Simulation modeling

### ABSTRACT

Understanding potential effects of climate warming on biogeochemical cycling in freshwater ecosystems is of pressing importance. Specifically, increasing air and water temperatures could accelerate nutrient cycling in lakes, which has major implications for in-lake nutrient concentrations, water column nutrient stoichiometry, and downstream nutrient export. Lakes may respond differentially to warming based on their current trophic state, although direct comparisons of temperature-driven changes in nutrient cycling between low- and high-nutrient lakes are lacking. Here, we used an open-source coupled hydrodynamic biogeochemical model to simulate ecosystem-scale changes in water column total nitrogen (TN) and total phosphorus (TP) concentrations and TN:TP ratios due to potential incremental changes in air temperature (from +0 °C to +6 °C) in a low-nutrient and a high-nutrient lake. Warming resulted in lower TN and higher TP epilimnetic (surface water) concentrations in both lakes, resulting in reduced molar TN:TP ratios in both lakes. While the high- and low-nutrient lakes had similar magnitude reductions in TN:TP ratio between the +0 °C and +6 °C scenarios (30.3% and 34.6%, respectively), median epilimnetic TN:TP in the low-nutrient lake significantly decreased with as little as 1 °C of warming. Warming also altered net nutrient retention, with decreased downstream export of TN but increased downstream export of TP in both lakes. Our modeling results suggest that low-nutrient lakes may respond to warming at lower levels of temperature increase than high-nutrient lakes, and that climate warming could intensify effects of nutrient enrichment driven by increased N and P loading due to land-use change.

### 1. Introduction

As sentinels of climate change (*sensu* Adrian et al., 2009), many lakes are warming rapidly (O'Reilly et al., 2015). Syntheses of satellite imagery and long-term in situ monitoring of lake temperatures worldwide indicate that there is widespread warming of lakes in response to air temperature changes, with surface water temperatures increasing in some cases by up to 1.3 °C per decade (O'Reilly et al., 2015; Richardson et al., 2017b). Climate models also suggest that warming air temperatures will increase the proportion of lakes in the continental United States that experience prolonged periods of water temperatures in excess of 30 °C (Butcher et al., 2017, 2015), with implications for habitat suitability, food web dynamics, and biogeochemical cycling (Butcher et al., 2015; Magee et al., 2019; Sahoo et al., 2013;

Wilhelm and Adrian, 2008; Winder et al., 2009). Consequently, it is important to identify the effects of warming air temperatures on lake ecosystem function.

Warming air temperatures can potentially affect lake nutrient concentrations – including nitrogen (N) and phosphorus (P) – through multiple interacting ecosystem processes. Previous field survey and lake ecosystem modeling studies have demonstrated that as air temperatures increase, density differences between surface and bottom water layers can become more pronounced, increasing the stability of the water column, and resulting in longer and more intense lake thermal stratification (Adrian et al., 2009; Foley et al., 2012; Kraemer et al., 2015; Richardson et al., 2017b). Longer and stronger periods of stratification often result in prolonged periods of hypoxia (dissolved oxygen < 2 mg L<sup>-1</sup>) in the bottom waters (Foley et al., 2012; Jiménez

\* Corresponding author.

E-mail address: [kfarrell@uga.edu](mailto:kfarrell@uga.edu) (K.J. Farrell).

<sup>1</sup> Present address: MIT-WHOI Joint Program in Oceanography/Applied Ocean Science & Engineering, Cambridge and Woods Hole, MA, USA

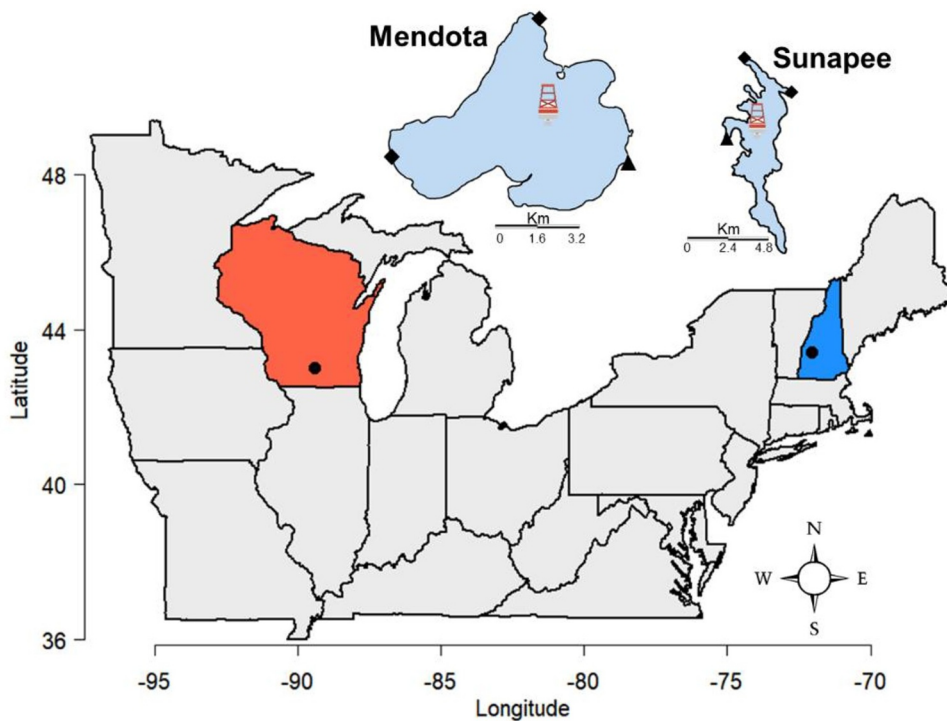


Fig. 1. Map showing within-state locations (points) of Lake Mendota (Wisconsin, USA, shown in red) and Lake Sunapee (New Hampshire, USA, shown in blue); insets show lake shape, the location of each lake's high-frequency buoy (buoy icon), and the dominant surface inflows (diamonds) and outflow (triangle). (For interpretation of the references to color in this figure legend, the reader is referred to the web version of this article.)

Cisneros et al., 2014; Marcé et al., 2010). Low oxygen in turn can promote the release of dissolved P and ammonium ( $\text{NH}_4^+$ ) from the sediments into the water column, while simultaneously decreasing nitrate ( $\text{NO}_3^-$ ) via denitrification (Stumm and Morgan, 1996; Wetzel, 2001). Increasing temperatures can also alter nutrient concentrations more directly, as phytoplankton growth rates and corresponding dissolved nutrient uptake generally increase with temperature (Reynolds, 2006). Warmer temperatures can also directly accelerate water column mineralization, thereby increasing nutrient concentrations (Stumm and Morgan, 1996).

Interacting processes are difficult to disentangle at the ecosystem scale, especially across a range of air temperature changes, which has motivated two decades of microcosm and mesocosm experiments (reviewed by Fordham, 2015). This work has provided important insights to the effect of warming on individual ecological mechanisms. However, simultaneous consideration of these interacting processes is needed to understand the balance of N and P at the ecosystem scale, necessitating other research approaches. Process-based numerical simulation models allow for specific drivers and pathways to be isolated within complex ecosystems (e.g., Gal et al., 2009; Snorheim et al., 2017); for example, holding external nutrient loads from the catchment constant under multiple air temperature scenarios isolates the effects of temperature on solely within-lake processes. Similarly, setting static Arrhenius parameters (temperature-driven rate constants that control the response of biogeochemical rates to temperature; Arrhenius, 1889) ensures that the temperature-dependence of different processes is identical among climate scenarios, lakes, and nutrients, allowing us to study their relative importance in model space. Finally, modeling total N and total P rather than individual constituents incorporates changes in dissolved and particulate nutrients that occur due to phytoplankton uptake and remineralization, which are included in the total nutrient fraction.

Because of the multiple interacting mechanisms by which air temperature can alter nutrient transformations, it is challenging to predict the net effect of warming on ecosystem-scale N and P cycling in lakes, which will subsequently alter downstream export of nutrients. Increasing air temperature will have multiple indirect effects on lakes and their catchments, such as changing the water temperature and

nutrient mineralization rates of inflow streams (Jeppesen et al., 2010). However, examining the *direct* effects of air temperature change represents an important first step for understanding lake biogeochemical responses to climate change. Specifically, it is possible that nutrient cycling in low-nutrient lakes may exhibit greater sensitivity to the direct effects of warming than in high-nutrient lakes (Collins et al., 2019). For example, as warming increases the duration and intensity of thermal stratification in a low-nutrient lake, it may induce bottom-water hypoxia for the first time, which would in turn initiate internal N and P loading from the sediments into the water column, representing a fundamental change to the lake's biogeochemistry and ecosystem functioning (Beutel and Horne, 2018). In comparison, it is possible that any warming-induced increase in the duration of hypoxia and intensity of internal loading in high-nutrient lakes may primarily reinforce the existing high-nutrient state. High-nutrient lakes tend to already experience hypoxia under current climatic conditions, and the baseline nutrient mineralization and sediment release rates are likely already high, though we are unaware of any previous study that has directly demonstrated this mechanism.

Here, we used eleven years of observational data to calibrate and validate a coupled, one-dimensional hydrodynamic and biogeochemical lake model for a low-nutrient lake and a high-nutrient lake. We used the calibrated models to estimate the effects of different climate warming scenarios on each lake's N and P cycling and export, focusing on ecosystem-scale responses. Specifically, we quantified the direct net effects of climate warming on the timing and duration of hypoxia and coincident changes in surface water N and P concentrations to improve our understanding of how nutrient cycling in the two lakes may change with warming temperatures. We also quantified how warming may alter lake nutrient retention and downstream export, which have important implications for water quality in the larger catchment. Biogeochemical cycling in low-nutrient lakes is generally understudied relative to high-nutrient lakes, despite a rapid decline in the number of low-nutrient lakes across the continental U.S. (Stoddard et al., 2016); this provides additional motivation to understand how trophic state mediates responses to warming. Thus, comparing N and P dynamics in two lakes of different trophic state under a range of temperature warming scenarios advances our understanding of ecosystem-scale

**Table 1**  
Physical and chemical characteristics of focal lakes.

Characteristic	Mendota	Sunapee
Latitude	43.10	43.38
Longitude	-89.65	-72.03
Watershed area (km <sup>2</sup> )	593 <sup>1</sup>	123 <sup>5</sup>
Lake area (km <sup>2</sup> )	39.6 <sup>1</sup>	16.6 <sup>5</sup>
Watershed:lake area ratio	15.0	7.4
Mean depth (m)	12.7 <sup>1</sup>	11.2 <sup>5</sup>
Residence time (years)	4.4 <sup>1</sup>	3.1 <sup>5</sup>
Lake volume (10 <sup>6</sup> m <sup>3</sup> )	5.03 <sup>2</sup>	1.86 <sup>2</sup>
Mean air temperature ( °C)	8.61 <sup>3</sup>	7.19 <sup>3</sup>
Mean summer epilimnetic total nitrogen (µg L <sup>-1</sup> )	960 <sup>4</sup>	170 <sup>4</sup>
Mean summer epilimnetic total phosphorus (µg L <sup>-1</sup> )	85 <sup>4</sup>	5.3 <sup>4</sup>

<sup>1</sup> Lathrop and Carpenter 2014.

<sup>2</sup> Lake area (m<sup>2</sup>) × mean depth, following Solomon et al. (2013).

<sup>3</sup> NLDAS-2 for 2003–2014.

<sup>4</sup> Solomon et al., 2013.

<sup>5</sup> Richardson et al., 2017a.

responses to future warming beyond a single-lake or single-scenario study and highlights the importance of historical nutrient baselines for predicting future ecosystem conditions.

## 2. Methods

### 2.1. Modeled lakes

We modeled lake responses to climate warming based on two well-studied north temperate lakes, Lake Mendota (Wisconsin, USA) and Lake Sunapee (New Hampshire, USA; Fig. 1). These two lakes share multiple common characteristics, including glacial origin, climate seasonality (due to similar latitude), a dimictic mixing regime, and inflows dominated by surface water (Table 1, Cobourn et al., 2018). In addition, the lakes have similar mean depths and water residence times (Table 1). The lakes also differ in watershed land use, which contributes to substantial differences in lake water nutrient concentrations (Table 1). The Mendota watershed is large relative to the lake area, and is dominated by agriculture (67%) and urban development (22%), which deliver large N and P loads to the lake and contribute to Mendota's high-nutrient state (Cobourn et al., 2018; Snorheim et al., 2017). In contrast, the Sunapee catchment is relatively small compared to the lake surface area, and is 80% forested, with only 6% currently developed (Richardson et al., 2017a). Nutrient inputs to the lake are low, resulting in Sunapee's low-nutrient state (Carey et al., 2014). Given their contrasting nutrient concentrations, these two lakes serve as approximate end members on a continuum of trophic state.

Rather than simulating simplified imaginary model ecosystems (e.g., identical lakes with hemispherical basins and no inflow tributaries), we used Lakes Mendota and Sunapee for this study because we needed their rich long-term monitoring datasets to ensure that our parameterized models were appropriately capturing baseline conditions for a high- and low-nutrient lake. In addition, we used air temperature warming scenarios of up to 6 °C based on downscaled data for these two lakes, vs. simulated air temperature scenarios based on global averages. After the models representing Mendota and Sunapee were calibrated with observational data, we focused on these two lake models as idealized high-nutrient and low-nutrient ecosystems, respectively, to examine potential responses to climate warming for temperate lakes of different baseline water quality.

### 2.2. Model description and driver data

We used the open-source, one-dimensional hydrodynamic General Lake Model (GLM version 2.1.8; Hipsey et al., 2014, 2019) to model the energy and water budget of each lake. The Aquatic EcoDynamics

library (AED; Hipsey et al., 2013) was coupled with GLM (hereafter, GLM-AED) to model water quality dynamics, including changes in concentrations of dissolved oxygen (DO), N, and P. We chose GLM-AED because it has dynamic vertically-resolved layers within a lake, which allows for comparisons of stratified biogeochemical processes (Hipsey et al., 2019). Moreover, the heat transfer and mixing algorithms in GLM, developed by Hamilton and Schladow (1997) have been found to successfully reproduce observed water temperatures of lakes with varying conditions (e.g., mixing regime, climate, latitude, morphology) around the world (Bruce et al., 2018).

GLM-AED is particularly suited for studying how climate warming may alter ecosystem-scale lake nutrient cycling because it is able to simultaneously simulate lake stratification dynamics and a suite of interacting N and P processes (Bruce et al., 2018; Hipsey et al., 2019, 2013). These biogeochemical processes include nitrification; denitrification; sediment fluxes of NO<sub>3</sub><sup>-</sup>, NH<sub>4</sub><sup>+</sup>, phosphate (PO<sub>4</sub><sup>3-</sup>), dissolved organic P (DOP), dissolved organic N (DON), particulate organic P (POP), and particulate organic N (PON); PO<sub>4</sub><sup>3-</sup> adsorption/desorption; DON, DOP, PON, and POP water column mineralization; NO<sub>3</sub><sup>-</sup>, NH<sub>4</sub><sup>+</sup>, and PO<sub>4</sub><sup>3-</sup> phytoplankton uptake; zooplankton excretion of DON, DOP, PON, and POP; and the settling rate of all N and P fractions (Hipsey et al., 2013). All of these processes will directly respond to warming temperatures because the underlying model equations include Arrhenius parameters governing their temperature dependence, hence the need for an ecosystem modeling approach to address our study's objectives (Hipsey et al., 2019).

The GLM-AED combines lake morphometry with meteorological and inflow driver data to simulate a water budget and thermal profile for each lake. We compiled observed hourly meteorological driver data for each lake from the North American Land Data Assimilation System (NLDAS-2). These data included air temperature (°C), wind speed (m s<sup>-1</sup>), relative humidity (%), shortwave and longwave radiation (W m<sup>-2</sup>), and precipitation (m d<sup>-1</sup>) for the full model period. We used a combination of observational and statistically-modeled data to develop a daily time series for the surface inflows to each lake, which included tributary inflow rates (m<sup>3</sup> s<sup>-1</sup>), inflow water temperature (°C), and inorganic and organic fractions of N and P (mmol m<sup>-3</sup>; see Supplement A for lake-specific inflow data sources and model simulations). We included eight different P and N fractions in our inflow files: filterable reactive P (FRP), adsorbed FRP, DOP, POP, NO<sub>3</sub><sup>-</sup>, NH<sub>4</sub><sup>+</sup>, DON, and PON. Inflow data also included two fractions of organic carbon: particulate and dissolved. Each lake model included a single outflow discharge file at a daily time step (Supplement A).

We ran each lake model at an hourly time step over an eleven-year period from 8 November 2003 to 31 December 2014. We chose this period because it represents the most complete time series of high-frequency observational data for both lakes and encompasses a representative range of climatic events for each modeled lake, including both flood and drought periods and particularly cool and warm years. In addition, the length of the model runs allows for integration of background meteorological variability that occurs over time.

### 2.3. Baseline calibration and validation

We calibrated the baseline GLM-AED model for each lake using the 7-year period from 1 April 2004 – 31 December 2010, and validated model state variables using the 4-year period from 1 January 2011 – 31 December 2014. The model “spin-up” period was from 8 November 2003 through 31 March 2004, meaning we did not analyze model outputs prior to 1 April 2004. During calibration, we manually changed model parameters for each lake with the goal of sequentially optimizing goodness-of-fit (GOF) metrics for a suite of focal state variables (water balance, water temperature, DO, N, P), with a focus on reproducing seasonal patterns and peak timing for each state variable (following Kara et al., 2012). Lake-specific calibration focused on parameters related to lake morphometry and physical mixing, nutrient fluxes at the

sediment-water interface, and settling rates of organic C, N, and P.

Importantly, almost all other parameter values governing water column biogeochemical processes (e.g., all Arrhenius temperature multipliers, half-saturation O<sub>2</sub> concentrations governing biogeochemical fluxes, and maximum aerobic mineralization rates for organic C, N, and P) were set as identical between lakes, so that the only parameters that differed between the two models were related to inherent differences in trophic state (e.g., higher sediment PO<sub>4</sub><sup>3-</sup> release rates in the high-nutrient lake than the low-nutrient lake; Tables A2, A5). We used a general set of parameters to represent phytoplankton and zooplankton groups in both lakes (following Hipsey et al., 2013), because phytoplankton and zooplankton were not the focus of this analysis.

Model outputs of water temperature, DO, total nitrogen (TN) and total phosphorus (TP) were compared to both low-frequency manual water samples (up to twice monthly) and high-frequency buoy data (hourly from April – October each year) collected from the deepest point in each lake (Supplement A). Lake Sunapee buoy data were collected by the Lake Sunapee Protective Association (LSPA; Richardson et al., 2020) and Lake Mendota data were collected through the North Temperate Lakes Long Term Ecological Research (NTL-LTER) site (Magnuson et al., 2010a, 2010b, 2010c, 2010d). For both lakes, we compared observed maximum daily water temperature and mean daily DO concentrations from both manual and buoy measurements to modeled daily noon water temperatures and DO concentrations (Supplement A; Magnuson et al., 2010a, 2010b). Manual samples of TN and TP were available up to twice monthly (Sunapee: Carey et al., 2014; Steiner and Titus, 2017; Mendota: Magnuson et al., 2010a, 2010d), and were compared to mean daily model outputs for each lake (Supplement A).

We calculated four GOF metrics to compare model outputs and observational data: coefficient of determination (R<sup>2</sup>), root mean square error (RMSE), Spearman's rank correlation coefficient (Spearman's rho [ρ]), and normalized mean absolute error (NMAE; Kara et al., 2012) using the hydroGOF package for R (Zambrano-Bigiarini, 2017). Separate GOF calculations were made for the epilimnion (0–4 m, both lakes) and hypolimnion (16–20 m, both lakes). We focused on these layers to compare representative epilimnetic and hypolimnetic depths between the two lakes; using different layer depths yielded qualitatively similar results. We chose to use layers instead of discrete depths for calibration and validation to maximize available manual observational data for comparison with model output. Evaporation effects on the lakes' water levels were negligible relative to precipitation, permitting the use of the same layer depths over time and among scenarios within lakes (Figure A1).

## 2.4. Climate warming simulations

To model changes in lake nutrient dynamics with climate warming, we ran a suite of downscaled climate warming scenarios (ranging from +0 to +6 °C above 2003–2014 air temperatures) for each lake. The scenarios were developed to encompass the maximum range of potential warming above historical 1950–1980 conditions projected for the lakes in year 2099, based on MACAv2-METDATA downscaled global climate models (Abatzoglou, 2013; Abatzoglou and Brown, 2012; Taylor et al., 2012). For Lake Mendota, maximum air temperature warming of approximately 5.4 °C is projected by 2099 under RCP8.5 relative to historical conditions, while Lake Sunapee is projected to warm by approximately 5.7 °C by 2099. We applied these potential warming air temperature scenarios to the historical 2003–2014 period and held all other meteorological driver variables constant to compare scenario output with the baseline 2004–2014 simulation output. While these simplified scenarios did not include the weather variability expected with future climate change (e.g., Hayhoe et al., 2008, 2010), it allowed us to isolate the direct effects of different levels of potential air temperature warming on ecosystem-scale lake nutrient cycling.

Because it is computationally intensive to model a range of climate

scenarios for multiple lakes, we implemented a distributed computing platform (GRAPLER; [www.graple.org](http://www.graple.org)) that enables users to run lake model simulations, submitted from the R environment, on cloud computing and cyber infrastructure resources (Subratie et al., 2017a). Simulations are distributed across processing nodes that have been aggregated into a peer-to-peer overlay virtual private network (Subratie et al., 2017b), dramatically reducing computation time.

## 2.5. Data analysis

Model outputs of focal state variables in each climate warming scenario were compared to the baseline simulation, with a focus on the period between 1 April and 31 October each year (henceforth, “summer”), which includes spring mixing, summer thermal stratification, and fall mixing in both lakes (Figure A2, A3). By comparing the scenario model outputs to the baseline model output, not observational data, our analyses focused on the temperature responses of idealized high- and low-nutrient lakes based on Mendota and Sunapee, respectively. We focused primarily on the differences between the baseline (+0 °C) and +6 °C scenarios to examine the direct effects of a range of warming possibilities on nutrient cycling in the selected lakes.

We first calculated daily Schmidt stability (J m<sup>-2</sup>) for each lake across warming scenarios to test whether air temperature warming increased water column stratification, using the Lake Analyzer tools (Read et al., 2011) in MATLAB version R2018b (MathWorks, Natick, MA, USA). We then summarized daily estimates of stability as summer medians each year in the 2004–2014 modeling period and used those values to compare the range and overall (among-year) summer median stability across scenarios. We calculated stratification duration as the number of days for which water temperatures between the surface (0 m) and hypolimnion (20 m in Mendota, 18 m in Sunapee) differed by more than 1 °C, following Woolway et al. (2014) and based on historical monitoring data for both lakes, which show that this threshold reasonably delineates mixed vs. stratified periods. These depths were chosen based on hypsographic curves and represent the hypolimnetic depth that encompasses approximately 80% of the sediment area in each lake.

To quantify the incidence of hypoxia, we calculated the number of days each summer (1 April – 31 October) for which hypolimnetic DO concentrations (20 m in Mendota, 18 m in Sunapee) were < 2 mg L<sup>-1</sup>. We then compared the median number of hypoxic DO days for each summer and its range among warming scenarios for each lake. We calculated median concentrations for epilimnetic (0 m, both lakes) and hypolimnetic (20 m in Mendota, 18 m in Sunapee) TN (μg L<sup>-1</sup>), TP (μg L<sup>-1</sup>), and median molar TN:TP each summer. We then used Anderson-Darling statistical tests (Razali and Wah, 2011) to make pairwise comparisons between the distributions of each response variable (TN, TP, TN:TP) across the 11-year model period (2004–2014) between each incremental climate warming scenario and the baseline distribution. We also compared model outputs of denitrification, NH<sub>4</sub><sup>+</sup> mineralization, and PO<sub>4</sub><sup>3-</sup> fluxes at the sediment-water interface among scenarios to assess potential mechanisms for changes in TN and TP concentrations.

Finally, we estimated net fluxes of TN and TP as a percent of inputs each summer for both lakes following Powers et al. (2015):

$$F_{\text{net\_summer}} = 100 \times (\sum \text{Outputs} - \sum \text{Inputs}) / \sum \text{Inputs}$$

where Outputs and Inputs represent the daily mass of TN or TP leaving and entering the lake, respectively, during the period of 1 April to 31 October each year. Daily stream inflow concentrations of TN and TP constituents were summed to calculate daily inflow TN and TP, then multiplied by daily inflow volume to yield the daily mass of TN and TP inputs. Daily median epilimnetic TN and TP concentrations were multiplied by outflow volume to calculate the mass of TN and TP outputs as both lake's outflows are composed of surface water. Daily inputs and

**Table 2**

Goodness-of-fit (GOF) metrics (coefficient of determination [ $R^2$ ], root mean square error [RMSE], Spearman's rank correlation coefficient [ $\rho$ ], normalized mean absolute error [NMAE]) for key state variables in Lake Mendota and Lake Sunapee for the combined calibration and validation period (1 January 2004 – 31 December 2014). GOF metrics were calculated for two depths; the epilimnion (0–4 m) and hypolimnion (16–20 m) of each lake using manually collected (Manual) and/or seasonal high-frequency buoy (Buoy) data.

Variable	Depth	Observation	Mendota				Sunapee					
			n	$R^2$	RMSE	$\rho$	NMAE	n	$R^2$	RMSE	$\rho$	NMAE
Daily Maximum Temperature ( $^{\circ}\text{C}$ )	Epilimnion	Manual	163	0.97	1.37	0.98	0.06	45	0.79	1.39	0.88	0.05
		Buoy	1461	0.92	1.77	0.94	0.06	1263	0.98	1.06	0.99	0.04
	Hypolimnion	Manual	163	0.87	1.55	0.83	0.12	43	0.41	2.44	0.68	0.21
		Buoy <sup>A</sup>	1318	0.55	1.55	0.69	0.10	783	0.93	1.44	0.93	0.10
Daily Mean Dissolved Oxygen ( $\text{mg L}^{-1}$ )	Epilimnion	Manual	162	0.43	1.88	0.64	0.15	45	0.24	0.96	0.70	0.06
		Buoy <sup>B</sup>	1274	0.02	2.30	0.03	0.18	693	0.72	0.36	0.85	0.03
	Hypolimnion	Manual	162	0.82	2.49	0.90	0.33	43	0.33	2.34	0.62	0.22
		Manual	161	0.08	376	0.34	0.33	6	0.01	233	-0.09	1.69
Total Nitrogen ( $\mu\text{g L}^{-1}$ )	Hypolimnion	Manual	94	0.35	789	0.25	0.38	2	1.00	229	-1.00	1.10
	Total Phosphorus ( $\mu\text{g L}^{-1}$ )	Epilimnion	Manual	161	0.10	118	0.32	1.50	41	0.01	6	0.24
Hypolimnion		Manual	94	0.69	121	0.75	0.40	47	0.09	8	-0.33	1.23

<sup>A</sup> Sunapee hypolimnion buoy temperature based on deepest two meters of available buoy data (12–14 m).

<sup>B</sup> Buoy dissolved oxygen was only collected at 0.5 m (Mendota) or 1.0 m (Sunapee).

outputs were summed across the 1 April to 31 October period each year to estimate  $F_{\text{net,summer}}$ , with  $F_{\text{net,summer}} > 0$  signifying that the lake was a net source (downstream export) of TN or TP, and  $F_{\text{net,summer}} < 0$  indicating that the lake was a net sink (retention and/or removal) of N or P. All analyses except for the MATLAB Lake Analyzer calculations were conducted in R version 3.5.2 (R Core Team, 2019).

### 3. Results

#### 3.1. Model calibration

For both lakes, calibrated models of GLM-AED reasonably simulated observed dynamics in focal physical and chemical state variables in the baseline 2004–2014 simulation (Table 2, Figs. 3 and 4). Modeled water temperatures were generally within an RMSE of 2  $^{\circ}\text{C}$  for both lakes, with better fits for both manual and buoy data in the epilimnion than the hypolimnion (Figs. 3A, 4A). Dissolved oxygen RMSE was  $\leq 2.5 \text{ mg L}^{-1}$  for all depths and data sources in each lake (Figs. 3B, 4B). While there were fewer observations of N and P than temperature and DO, particularly in Lake Sunapee, model fits generally reproduced the seasonality and range of concentrations in both lakes (Table 2; Figs. 3C–D, 4C–D). Although the calibrated Sunapee model had higher bias for TP than Mendota (Table 2; Fig. 4D), we deemed the calibration acceptable because it minimized differences in parameterization of biogeochemical processes between the two lakes to enable comparison of temperature scenarios. Moreover, all subsequent analyses were focused on comparison of the scenario model outputs to the baseline model output, not observational data.

#### 3.2. Strength of stratification and duration of hypoxia increase with climate warming

Climate warming scenarios led to warming of the water column in both lakes (Fig. 5). Between the baseline ( $+0 \text{ }^{\circ}\text{C}$ ) and  $+6 \text{ }^{\circ}\text{C}$  air temperature scenarios, among-year median summer surface water temperatures increased in both lakes, with a 19.1% (3.8  $^{\circ}\text{C}$ ) increase from the baseline in the high-nutrient lake (individual year median change ranging from  $+3.1 \text{ }^{\circ}\text{C}$  to  $+4.1 \text{ }^{\circ}\text{C}$ ), and a 19.2% (3.6  $^{\circ}\text{C}$ ) increase in the low-nutrient lake (individual year change  $+3.3 \text{ }^{\circ}\text{C}$  to  $+4.0 \text{ }^{\circ}\text{C}$ ). The hypolimnion of each lake experienced less warming than the epilimnion overall between the baseline and  $+6 \text{ }^{\circ}\text{C}$  scenarios, but was more variable among years, with a 5.4% (0.7  $^{\circ}\text{C}$ ) increase from the baseline in the high-nutrient lake (individual year change  $-1.4 \text{ }^{\circ}\text{C}$  to  $+4.0 \text{ }^{\circ}\text{C}$ ), and a 12.5% (1.3  $^{\circ}\text{C}$ ) increase in the low-nutrient lake (individual year change  $+0.2 \text{ }^{\circ}\text{C}$  to  $+3.3 \text{ }^{\circ}\text{C}$ ).

Warmer surface water temperatures amplified thermal stratification in both lakes (Fig. 5): among-year median Schmidt stability between 1 April and 31 October increased 50% in the high-nutrient lake (individual year change:  $+5$  to  $+95\%$ ) and 57% in the low-nutrient lake (individual year change:  $+34$  to  $+105\%$ ) between the baseline and  $+6 \text{ }^{\circ}\text{C}$  scenarios (Fig. 6A). In addition, the year-to-year variability in Schmidt stability increased with warming, with the range of summer medians increasing  $2.1\times$  in the high-nutrient lake and  $1.1\times$  in the low-nutrient lake between the baseline and  $+6 \text{ }^{\circ}\text{C}$  scenarios (Fig. 6A). Along with intensifying stratification, the duration of stratification increased among scenarios, though the amount of change differed between lakes and was highly variable year-to-year. In the high-nutrient lake, among-year median stratification duration increased eight days (from 193 to 201 days) between the baseline and  $+6 \text{ }^{\circ}\text{C}$  scenarios (year-to-year range  $-35$  to  $+50$  days), with the average spring onset of stratification occurring seven days sooner, and fall turnover occurring one day later in the  $+6 \text{ }^{\circ}\text{C}$  scenario than in the baseline. In contrast, among years, the low-nutrient lake experienced spring onset three days sooner, and turnover four days later, resulting in a median change in stratification duration of seven days (from 205 to 212; year-to-year range  $-24$  to  $+42$  days).

Warming-induced changes in stability and stratification likely contributed to the observed increase in the extent and duration of low DO concentrations in the hypolimnion of both lakes (Fig. 7, 6B). Between the baseline ( $+0 \text{ }^{\circ}\text{C}$ ) and  $+6 \text{ }^{\circ}\text{C}$  scenarios, hypoxic DO concentrations in the hypolimnion occurred earlier in the year and lasted longer, resulting in more summer days with DO concentrations  $< 2 \text{ mg L}^{-1}$  (Fig. 6B). In the high-nutrient lake, there were up to  $1.1\times$  as many summer hypoxic days under the  $+6 \text{ }^{\circ}\text{C}$  scenario as the baseline (maximum 131 vs. 119 days per year, respectively). In the low-nutrient lake, effects on DO were much larger, and warming led to the development of prolonged hypolimnetic hypoxia for the first time, with up to 39 hypoxic days per summer under  $+6 \text{ }^{\circ}\text{C}$  warming, compared to a maximum of one hypoxic day per summer in the baseline simulation (Fig. 6B). In addition, more intense warming resulted in greater hypoxia in the low-nutrient lake: with  $+6 \text{ }^{\circ}\text{C}$  warming, summer hypoxia occurred in five of 11 simulation years, versus in only one of 11 simulation years for scenarios with up to  $+2 \text{ }^{\circ}\text{C}$  warming. As with stability, the year-to-year variability of hypoxia duration in the low-nutrient lake also increased with warming, with the range of medians increasing from one to 39 days between the baseline and  $+6 \text{ }^{\circ}\text{C}$  scenarios (Fig. 6B). In contrast, the range of medians was 41 days in the high-nutrient lake for both the baseline and  $+6 \text{ }^{\circ}\text{C}$  scenarios (Fig. 6B).

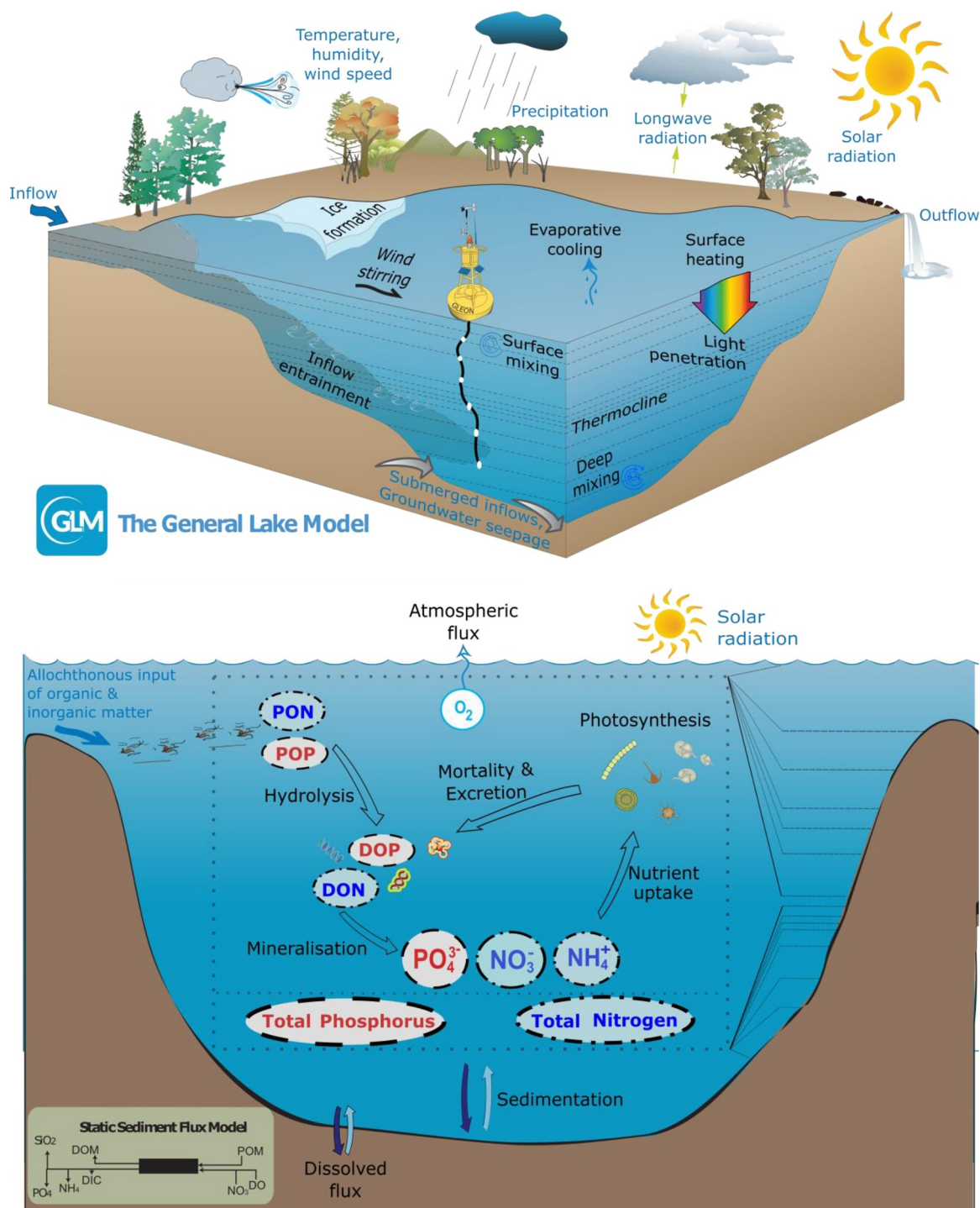


**Fig. 2.** Conceptual diagrams of the (A) General Lake Model (GLM; adapted from Hipsey et al., 2019) and (B) Aquatic EcoDynamics library (AED; adapted from Hipsey et al., 2013). Text indicates model inputs (blue) and model-simulated processes (black). (For interpretation of the references to color in this figure legend, the reader is referred to the web version of this article.)

**3.3. Epilimnetic TN and TP concentrations and stoichiometric ratios change with warming**

Climate warming had ecosystem-scale effects on nutrient cycling that resulted in altered epilimnetic TN and TP concentrations, though the magnitude of responses was lake-specific, and the direction of change differed between TN and TP. In both lakes, surface TN decreased between the baseline (+0 °C) and +6 °C scenarios. In the high-nutrient lake, the among-year median summer epilimnetic TN was 19.2% lower in the +6 °C scenario than in the baseline scenario

(Fig. 8A), with a statistically significant change in the distribution of median summer epilimnetic TN compared to the baseline simulation with warming of at least +5 °C (Table 3; Fig. 8A). The low-nutrient lake also exhibited decreased epilimnetic TN with climate warming; among-year median TN was 30.4% lower in the +6 °C scenario than in the baseline scenario. Importantly, in the low-nutrient lake, there was a statistically significant shift in the distribution of median summer TN relative to the baseline when warming was at least 2 °C (Table 3; Fig. 8A).

Decreased TN concentrations were likely driven by increased rates

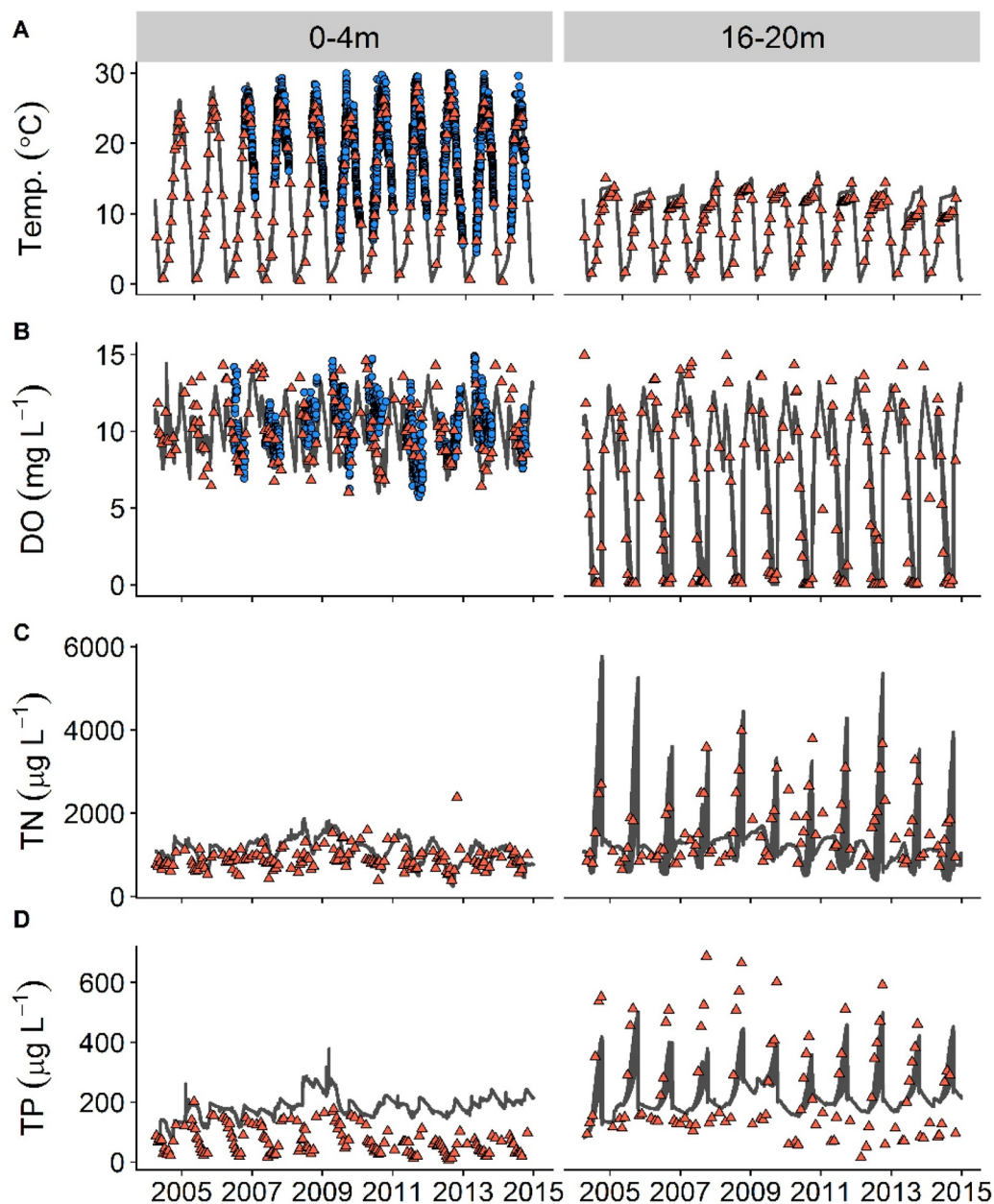


**Fig. 3.** Baseline modeled (solid lines) ecosystem state variables (A: water temperature (Temp.), B: dissolved oxygen (DO), C: total nitrogen (TN), D: total phosphorus (TP)) compared to observed manual measurements (triangles) and high-frequency buoy data (circles) in Lake Mendota epilimnion (0–4 m, left panels) and hypolimnion (16–20 m, right panels).

of denitrification with warming. Among-year median water column denitrification rates increased 45.0% and 37.6% in the high- and low-nutrient lakes, respectively, between the baseline and +6 °C scenarios. Warming also increased N-processing rates at the sediment-water interface in both lakes;  $\text{NH}_4^+$  fluxes from the sediments into the water column increased 42.7% and 35.1% in the high- and low-nutrient lakes, respectively, among years between the baseline and +6 °C scenarios. Among-year median denitrification rates at the sediment-water interface also increased, up 29.9% in the high-nutrient lake and 26.6% in the low-nutrient lake between the baseline and +6 °C scenarios.

In contrast to TN, both lakes exhibited increased epilimnetic TP concentrations in the +6 °C scenario compared to the baseline scenario, though the magnitude of change differed between lakes. In the high-nutrient lake, among-year median summer epilimnetic TP was 23.1% higher in the +6 °C scenario than in the baseline scenario (Fig. 8B), with a significant shift in the distribution of summer surface TP with

warming of +6 °C (Table 3). In the low-nutrient lake, among-year epilimnetic TP increased 8.9% between the baseline and +6 °C scenario (Fig. 8B), with significant shifts in the distribution of median summer TP with at least 2 °C of warming. These changes were attributed to increased P fluxes from the sediments with warming temperatures; median sediment fluxes increased 33.5% and 33.6% in the high- and low-nutrient lakes, respectively, between the baseline and +6 °C scenarios.

Lake-specific differences in TN and TP in response to warming led to differences in the epilimnetic N:P stoichiometry in both lakes, but the low-nutrient lake was more sensitive to low levels of warming. In the high-nutrient lake, among-year median epilimnetic molar TN:TP was 30.3% lower between the baseline and +6 °C warming scenarios (Fig. 8C), and the distributions of summer median TN:TP were significantly lower than the baseline with at least +4 °C of warming (Table 3). In the low-nutrient lake, the proportional shift in epilimnetic

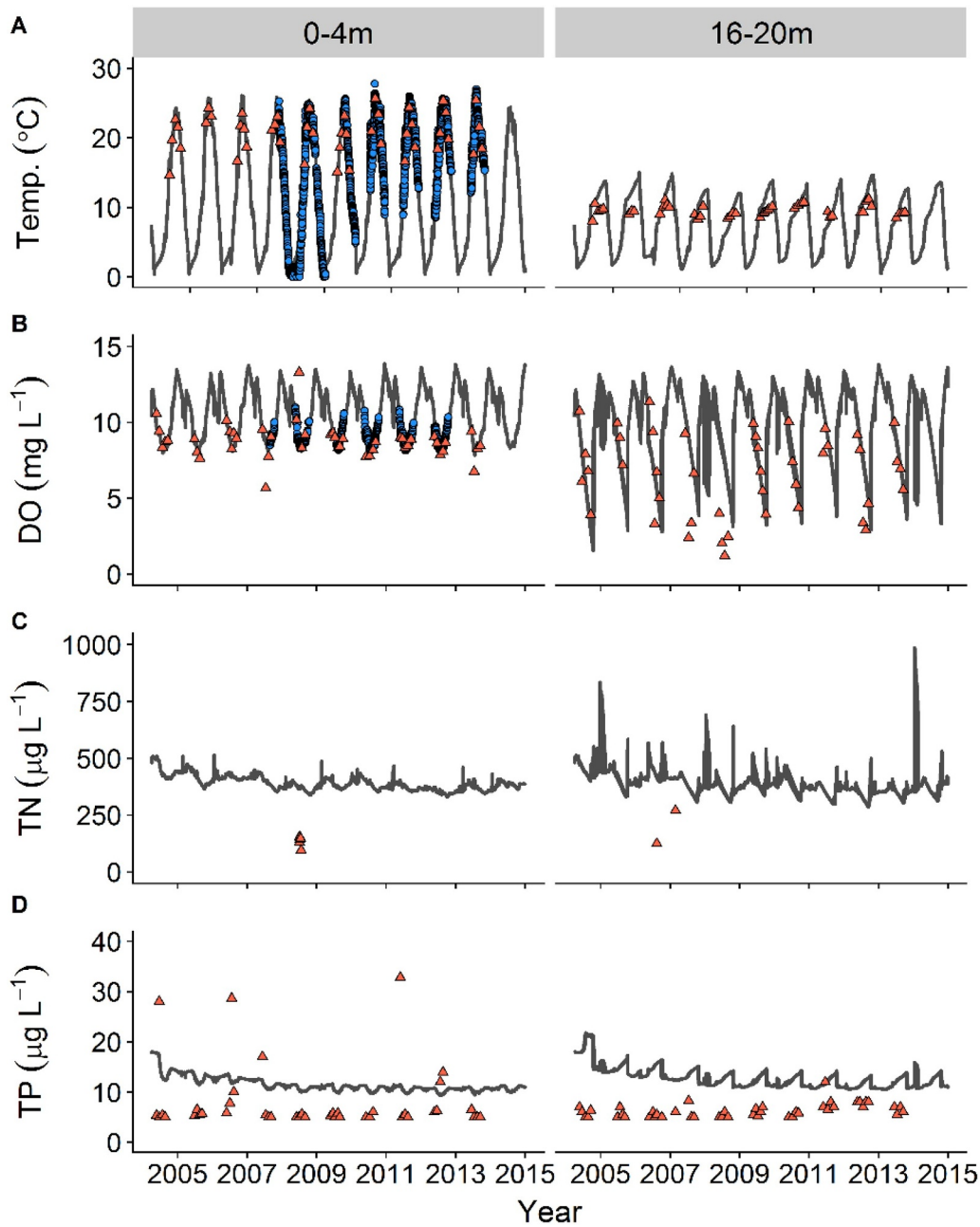


Fig. 4. Baseline modeled (solid lines) ecosystem state variables (A: water temperature (Temp.), B: dissolved oxygen (DO), C: total nitrogen (TN), D: total phosphorus (TP)) compared to observed manual measurements (triangles) and high-frequency buoy data (circles) in Lake Sunapee epilimnion (0–4 m, left panels) and hypolimnion (16–20 m, right panels).

TN:TP distribution was similar to that of the high-nutrient lake, with an among-year median reduction of 34.6% between the baseline and +6 °C scenarios. However, the distribution of TN:TP in the low-nutrient lake was shifted significantly lower than the baseline with as little as 1 °C of warming (Table 3; Fig. 8C).

### 3.4. Warming differentially changes net export of N and P

Warming generally decreased TN export but increased TP export downstream for both lakes during the summer (1 April – 31 October; Fig. 9). In the high-nutrient lake, among-year median summer TN export downstream decreased 2.2% between the baseline and +6 °C scenarios (individual year change –5.9% to +0.4%), while in the low-nutrient lake, TN export decreased 16.1% between the same scenarios (individual year change –24.6% to –3.5%), resulting in greater net N

retention and/or removal in both lakes during the summer. In both lakes, variability in TN export decreased with warming; the year-to-year range of summer export decreased 22.2% in the high-nutrient lake and 28.5% in the low-nutrient lake between the +0 °C and +6 °C scenarios. Both lakes remained net sinks of N (summer fluxes < 0) among years and across scenarios.

Both lakes exhibited lower net retention and greater downstream export of TP during the summer, with greater changes observed in the high-nutrient lake than the low-nutrient lake under warming scenarios. Among-year median TP export downstream in the high-nutrient lake increased 29.6% between the +0 °C and +6 °C scenarios (individual year change –4.2% to +170%). Net TP export in the high-nutrient lake exhibited high year-to-year variability in the baseline scenario (–71.0% to –16.7%), and the year-to-year range increased 57.8% between the +0 °C and +6 °C scenarios, with at least one year

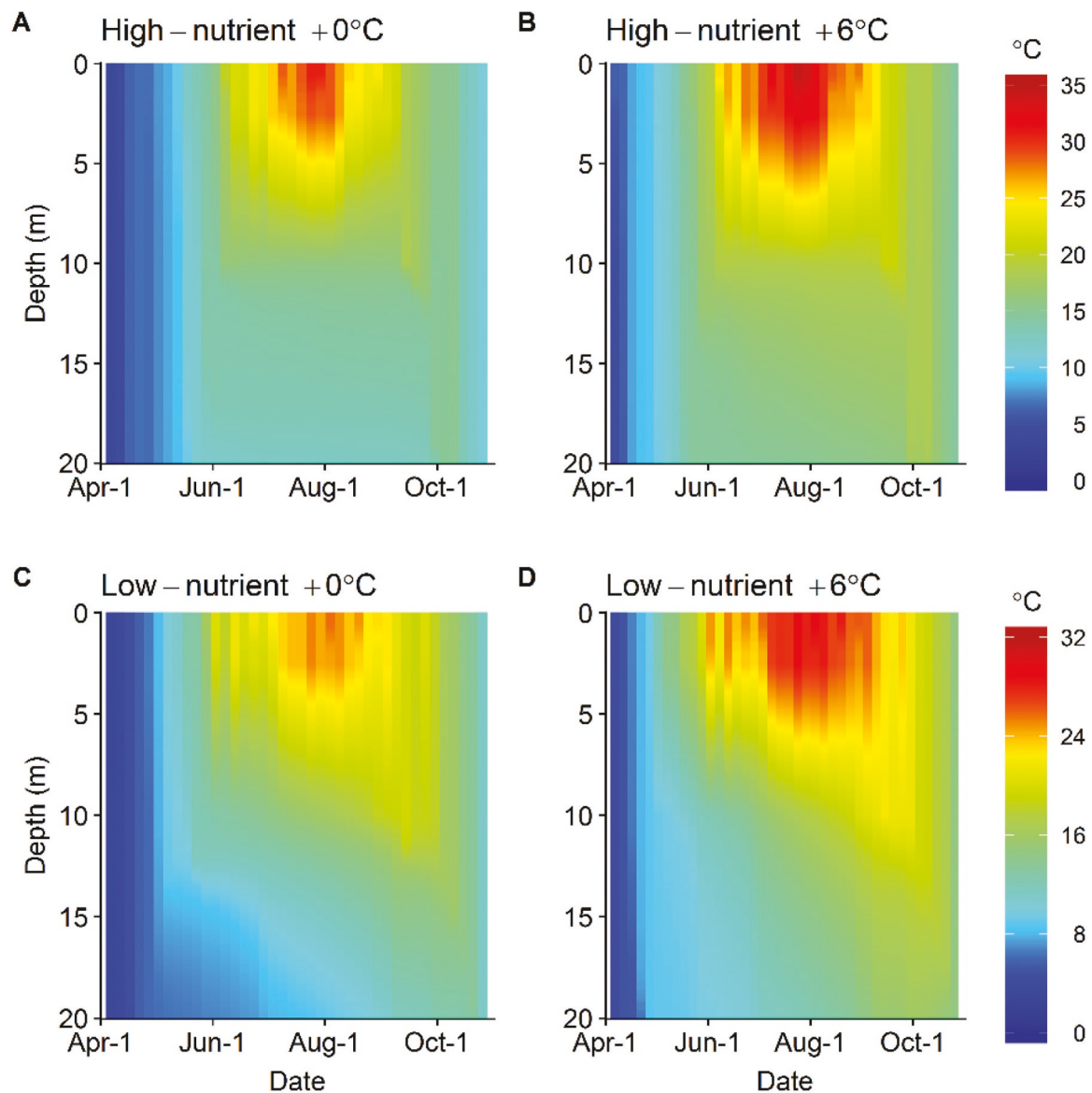


Fig. 5. Modeled water column temperatures ( $^{\circ}\text{C}$ ) in the high-nutrient lake (A, B) and the low-nutrient lake (C, D) under  $+0^{\circ}\text{C}$  (A, C) and  $+6^{\circ}\text{C}$  (B, D) air temperature warming scenarios, shown from 1 April to 31 October 2011 as an example year. Color scale shows water temperatures throughout the water column; note differences in maximum water temperature between the two lakes. (For interpretation of the references to color in this figure legend, the reader is referred to the web version of this article.)

estimated as a net source of P (summer export  $> 0$ ) with warming of at least  $+2^{\circ}\text{C}$  (Fig. 9). In the low-nutrient lake, TP export downstream increased, but much less than in the high-nutrient lake; 16.2% between the  $+0^{\circ}\text{C}$  and  $+6^{\circ}\text{C}$  scenarios (individual year change  $-1.6\%$  to  $+40.2\%$ ). Baseline year-to-year variability in TP export was also lower in the low-nutrient lake than in the high-nutrient lake ( $-38.9\%$  to  $-18.2\%$ ), and variability decreased slightly ( $-8.7\%$ ) between the  $+0^{\circ}\text{C}$  and  $+6^{\circ}\text{C}$  scenarios. Unlike the high-nutrient lake, the low-nutrient lake consistently acted as a net sink of P (summer export  $< 0$ ) across all warming scenarios and years.

## 4. Discussion

### 4.1. Ecosystem-scale effects of climate warming

Our study provides new evidence that ecosystem-scale nutrient cycling in both high- and low-nutrient lakes is sensitive to air temperature warming, though sensitivity likely varies by lake trophic state.

Specifically, low-nutrient lakes may experience significant changes in nutrient concentrations and stoichiometry at lower levels of warming than high-nutrient lakes. We observed lower TN and higher TP concentrations in both lakes as they warmed, but the low-nutrient lake exhibited significant changes in epilimnetic nutrients and TN:TP ratios at  $1\text{--}2^{\circ}\text{C}$  of warming, vs.  $5\text{--}6^{\circ}\text{C}$  of warming in the high-nutrient lake. Consequently, as the number of low-nutrient lakes is rapidly declining across the continental U.S. (Stoddard et al., 2016) due to increased N and P loading from ongoing land-use change and an increased incidence of extreme events delivering terrestrial nutrients and sediments (e.g., Kelly et al., 2019; Prein et al., 2017), our study demonstrates that climate warming may intensify lake eutrophication.

Our modeling study corroborates empirical data from field surveys, mesocosm experiments, and paleolimnological records that illustrate how climate warming can transform lake ecosystem functioning (reviewed by Havens and Jeppesen, 2018; Jeppesen et al., 2014; Moss, 2012). Other modeling studies that have used process-based, one-dimensional lake simulation models have shown how climate warming

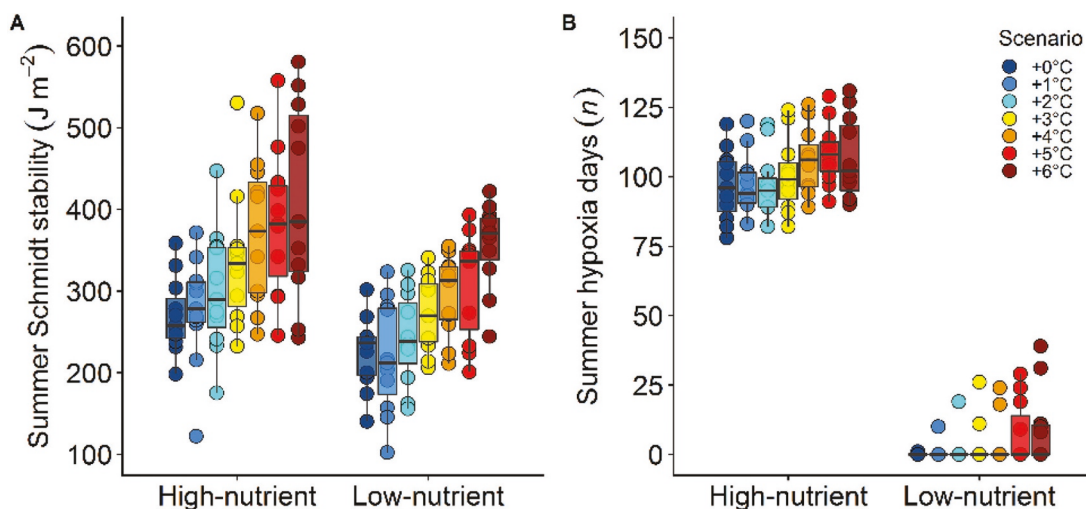


Fig. 6. Changes in modeled (A) Schmidt stability ( $J m^{-2}$ ) and (B) low dissolved oxygen ( $< 2 mg L^{-1}$ ) days under +0 °C to +6 °C air temperature warming scenarios for the high- and low-nutrient lakes. Points indicate median values for the period of 1 April to 31 October each year.

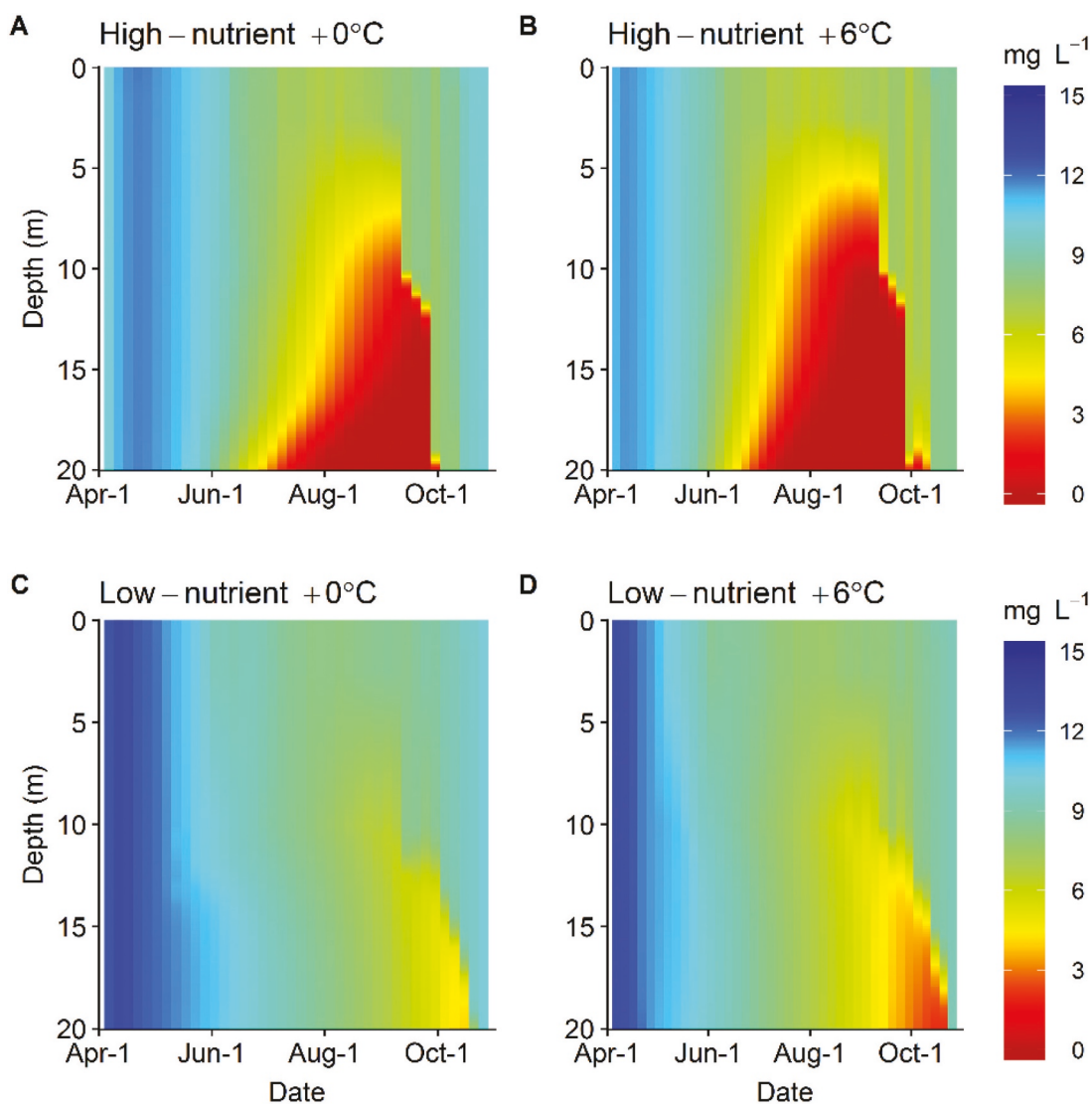
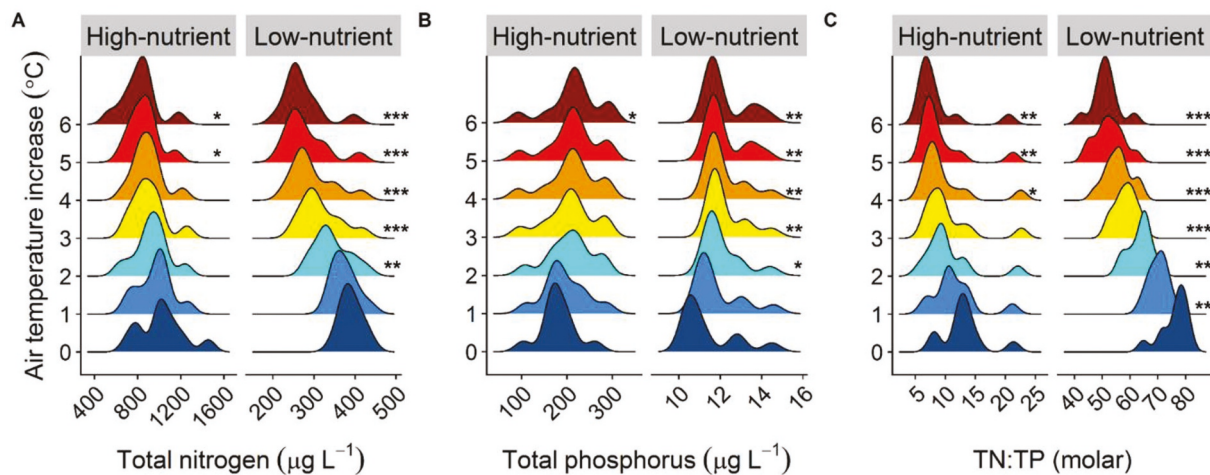


Fig. 7. Modeled water column dissolved oxygen ( $mg L^{-1}$ ) in the high-nutrient lake (A, B) and the low-nutrient lake (C, D) under +0 °C (A, C) and +6 °C (B, D) air temperature warming scenarios, shown from 1 April to 31 October 2011 as an example year. Color scale shows dissolved oxygen concentrations throughout the water column. (For interpretation of the references to color in this figure legend, the reader is referred to the web version of this article.)



**Fig. 8.** Distributions of among-year median epilimnetic (0 m) (A) total nitrogen (TN), (B) total phosphorus (TP), and (C) molar TN:TP for the high- and low-nutrient lakes across air temperature warming scenarios (+0 °C to +6 °C) for the period of 1 April to 31 October each year. Distributions for each temperature scenario are based on 11 model years per lake. Stars indicate significant differences in distributions between warming scenarios and the baseline simulation (+0 °C) as assessed by Anderson-Darling tests; \*  $p \leq 0.05$ , \*\*  $p \leq 0.01$ , \*\*\*  $p \leq 0.001$ .

**Table 3**

Results of Anderson-Darling tests for shifts in epilimnetic (0 m) nutrient distributions (total nitrogen [N], total phosphorus [P]) and nutrient ratios [molar N:P] between baseline (+0 °C) and each of the warming scenarios (+1 °C to +6 °C, denoted by Scenario Contrast) for the high-nutrient lake and the low-nutrient lake. The Anderson-Darling criterion (AD), standardized test statistic (T.AD), and *P*-values (asymptotic approximation) are reported for each pairwise scenario comparison. *P*-values in bold indicate significant ( $\alpha = 0.05$ ) shifts in the distribution; values in italics indicate marginal shifts ( $\alpha = 0.10$ ).

Scenario Contrast	Total Nitrogen			Total Phosphorus			Molar N:P		
	AD	T.AD	<i>P</i>	AD	T.AD	<i>P</i>	AD	T.AD	<i>P</i>
<b>High-nutrient lake</b>									
+1 °C	0.54	-0.66	0.75	0.71	-0.41	0.57	1.16	0.22	0.28
+2 °C	0.84	-0.23	0.46	1.72	1.02	0.12	2.21	1.72	0.06
+3 °C	1.52	0.75	0.16	1.46	0.65	0.18	2.15	1.64	0.07
+4 °C	2.11	1.58	0.07	2.12	1.60	0.07	3.15	3.06	0.02
+5 °C	2.50	2.14	0.04	2.29	1.84	0.06	4.14	4.48	0.006
+6 °C	2.60	2.28	0.04	2.67	2.38	0.03	5.03	5.74	0.002
<b>Low-nutrient lake</b>									
+1 °C	1.40	0.58	0.19	2.05	1.50	0.08	4.46	4.93	0.004
+2 °C	3.62	3.73	0.01	3.23	3.20	0.02	7.14	8.75	<0.001
+3 °C	5.50	6.41	0.001	3.55	3.63	0.01	8.52	10.72	<0.001
+4 °C	6.28	7.52	<0.001	3.55	3.63	0.01	8.52	10.72	<0.001
+5 °C	6.58	7.95	<0.001	3.55	3.63	0.01	8.52	10.72	<0.001
+6 °C	6.74	8.18	<0.001	3.55	3.63	0.01	8.52	10.72	<0.001

alters lake thermal profiles and mixing regimes (Bueche et al., 2017; Bueche and Vetter, 2015; Fenocchi et al., 2018; Woolway and Merchant, 2019), hypolimnetic anoxia (Fang et al., 2012; Ito and Momii, 2015; Snorheim et al., 2017; Stefan et al., 1993), and nutrient cycling (Arheimer et al., 2005; Komatsu et al., 2007; Malmaeus et al., 2006). Our study builds upon these earlier modeling analyses to add new evidence that lake nutrient concentrations, through linked biogeochemical processes, may change differentially across a range of potential air temperature warming scenarios depending on lake trophic state.

#### 4.2. Potential drivers of lake nutrient changes

The complexity and non-linearity of ecosystem processes makes it challenging to predict how changing external drivers due to altered climate (e.g., warming air temperature) may affect ecosystem functioning (Burkett et al., 2005; Parrott and Meyer, 2012; Shaver et al., 2000), necessitating our modeling approach. In lakes, N and P concentrations in surface waters are jointly controlled by external loading from the catchment, climate forcing, and internal nutrient cycling (Nürnberg, 1984; Stumm and Morgan, 1996; Wetzel, 2001), creating complex patterns in observational data that challenge our ability to link

cause and effect in empirical studies (reviewed by Carpenter, 1988). Following the precedent of previous modeling studies (e.g., Komatsu et al., 2007; Snorheim et al., 2017), we held external nutrient loads constant while manipulating air temperature driver data, thereby simplifying the inherent complexity of lake nutrient cycling to isolate the effects of climate warming on epilimnetic nutrients.

Our findings highlight the strong coupling between lake thermal structure and nutrient cycling, and how that coupling may vary between lakes of different trophic state. Warmer air temperatures lead to stronger thermal stratification, which further isolates hypolimnetic waters from the atmosphere, reducing the availability of oxygen for biogeochemical processing (Snorheim et al., 2017). While previous research has implied the importance of this mechanism for nutrient cycling (e.g., Pettersson et al., 2003; Sahoo et al., 2013), our results show that not only will warmer air temperatures promote hypolimnetic hypoxia, but will also reduce surface water TN while increasing TP. Due to the complexity of lake ecosystem simulations, these changes in nutrient concentrations cannot be attributed to a single process, but rather emerge from interactions of multiple processes in the model. We use the lake model as a calibrated experimental tool, linking drivers and physical/ecological processes that likely lead to the changing nutrient concentrations we observed in the model results. We show that the links

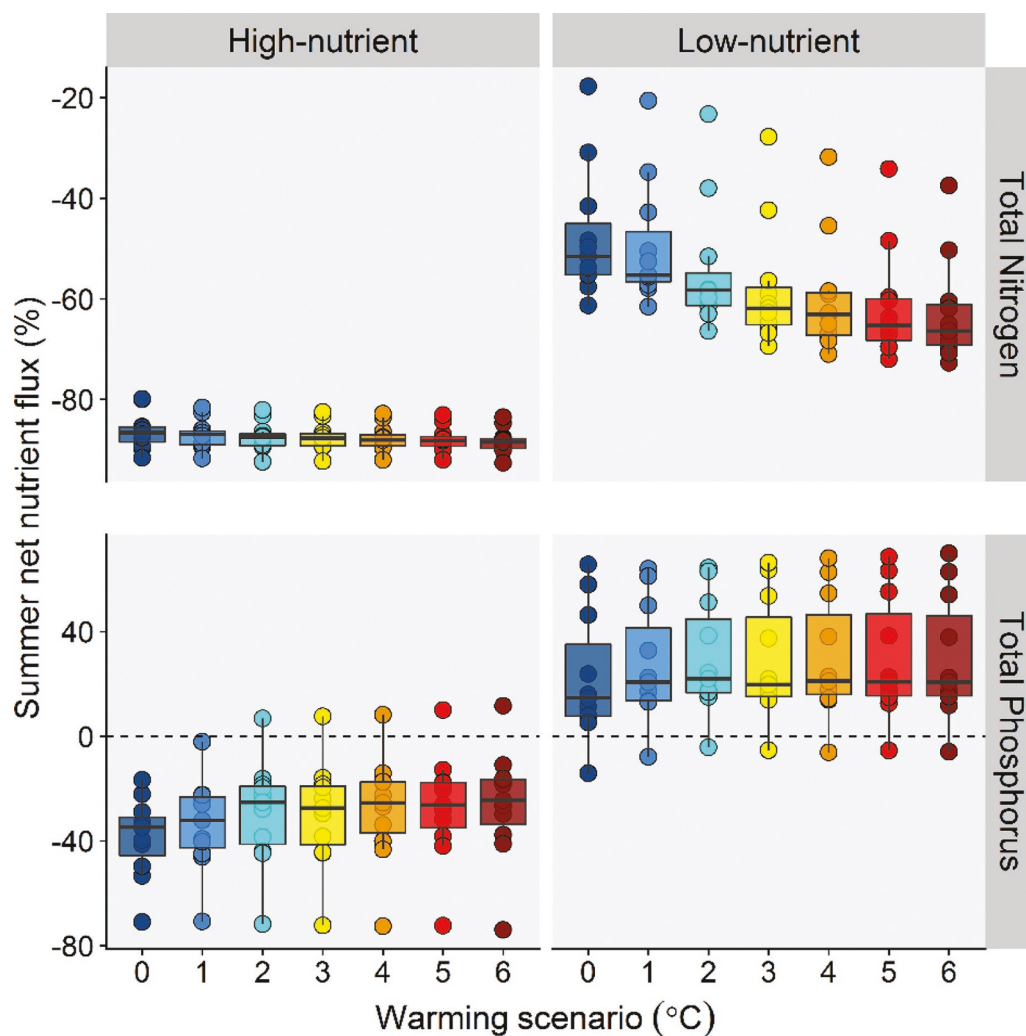


**Fig. 9.** Estimated net flux of total nitrogen (A, B) and total phosphorus (C, D) downstream as a percent of inflow N and P in the high-nutrient lake (A, C) and low-nutrient lake (B, D). Points indicate net flux (%) for the period of 1 April to 31 October each year; flux < 0 represents net retention and/or removal, flux > 0 represents net downstream export.

between thermal structure, hypoxia, and temperature-mediated biogeochemical cycling all are important to N and P concentrations in a warming climate, but their importance depends on lake characteristics.

Our data support previous findings that in the absence of changes to hydrology and external nutrient loading, warming alone can substantially alter lake thermal structure (Magee and Wu, 2017a; Palmer et al., 2014; Richardson et al., 2017b; Woolway and Merchant, 2019) and in turn, oxythermal habitat (Fang et al., 2012; Magee et al., 2019) and nutrient processing (Komatsu et al., 2007; Radbourne et al., 2019). In our scenarios, the hypolimnion warmed less than the epilimnion, but lake warming was more variable among years as air temperatures increased. This is consistent with previous research on lakes across the northeastern United States that found approximately half of lakes experience deepwater warming as air temperatures increase, while others experience deepwater cooling (Richardson et al., 2017b). Similarly, our models indicated that Schmidt stability and duration of stratification increased with warming, as was found in previous climate warming simulations based on lake “archetypes,” in which model lakes were conceptualized to encompass regionally-representative ranges of lake depth, surface area, and water clarity (Butcher et al., 2015).

The observed decreases in TN concentrations associated with warming are likely related to greater hypoxia and subsequent N removal from the lakes by denitrification. Previous empirical surveys of

water chemistry across latitudinal gradients showed greater N limitation in warmer, tropical lakes that are thermally stratified most of the year, with increased denitrification potential driven by reduced oxygen availability in warmer hypolimnia (Lewis Jr. 1996 and references therein, Lewis Jr. 2002, Talling and Lemoalle 1998). Our modeling results show that lakes can exhibit a similar change in N cycling in a warming climate. In the warmest scenario, there were over  $10\times$  more days per year with hypoxia in the low-nutrient lake than under baseline conditions and  $1.1\times$  as many days with hypoxia in the high-nutrient lake, increasing  $\text{NO}_3^-$  removal from the water column by 38% in the low-nutrient lake and 45% in the high-nutrient lake relative to baseline rates. This increased rate of N removal exceeded higher rates of  $\text{NH}_4^+$  mineralization (up 43% and 35% in the high- and low-nutrient lakes, respectively) from the sediments due to warmer waters, resulting in net TN decreases.

Increased TP concentrations in both lakes in our study likely relate to increases in hypolimnetic hypoxia ( $\text{DO} < 2 \text{ mg L}^{-1}$ ). While hypolimnetic anoxia ( $\text{DO} \sim 0 \text{ mg L}^{-1}$ ) is an established mechanism for stimulating the release of P bound in sediments into the water column (Nürnberg, 1984; Wetzel, 2001), it is less well-understood how changes in hypoxia may affect surface water nutrient concentrations. Previous empirical studies have shown that hypoxia can increase P fluxes from the sediments and subsequent downstream export (Gerling et al., 2016), even in low-nutrient lakes (North et al., 2014). Our modeling results

suggest a similar behavior in lakes experiencing warming. Lakes in our study had increased incidence of hypoxia, which created low DO conditions in the hypolimnion that increased P fluxes from the sediments into the water column. At +6 °C warming, fluxes of P from the sediments were 34% higher than baseline rates in both lakes. Interestingly, although our analysis focused on the differences between the baseline (+0 °C) scenario and +6 °C potential warming scenario, the physical and chemical responses of both lakes appeared to be mostly linear for intermediate warming scenarios (Figs. 5, 8, and 9).

As noted above, we cannot precisely quantify the relative importance of thermal stratification, decreases in hypolimnetic oxygen, or temperature-mediated nutrient cycling rates on surface TN and TP, as these processes are strongly interconnected and occur simultaneously within the model. More empirical data from years with contrasting air temperature and hypolimnetic oxygen conditions could be used to disentangle these drivers. Additionally, future work implementing a two- or three-dimensional coupled hydrodynamic-ecosystem model could be used to identify hotspots of N and P biogeochemical cycling within each lake ecosystem (sensu Bocaniov et al., 2016; Cavalcanti et al., 2016), thereby informing the relative importance of oxygen, thermal stratification, and water temperature.

#### 4.3. Differences in warming response between a high-nutrient and a low-nutrient lake

Our models of Lake Mendota and Lake Sunapee enable comparisons of idealized high- and low-nutrient lakes as a first step toward understanding how the net direct effects of warming on TN and TP cycles in lakes may differ across trophic states. Across our warming scenarios, we found that the magnitude of relative changes in TN:TP ratios tended to be similar between the two lakes, though reductions in TN were substantially higher in the low-nutrient lake than the high-nutrient lake, while TP increases were proportionally larger in the high-nutrient lake than the low-nutrient lake. The most notable difference between lakes was the temperature increase at which nutrient concentrations and ratios exhibited statistically significant changes: in the high-nutrient lake, TN, TP, and TN:TP were significantly different from baseline conditions at +5 °C, +6 °C, and +4 °C, respectively. In contrast, the low-nutrient lake experienced significant changes in TN, TP, and TN:TP at +2 °C, +2 °C, and +1 °C, respectively. This consistently lower threshold for responses suggests that ecosystem-scale processes in the low-nutrient lake may be fundamentally more sensitive to warming air temperatures, which aligns with predictions that high-nutrient lakes may have more muted responses to climate warming (Collins et al., 2019).

These results highlight the value of using decadal-scale ecosystem models coupled with long-term data to understand potential implications of climate warming on lake ecosystems. Our 11-year model period allowed for the detection of overall trends in TN and TP cycling in both lakes, despite substantial year-to-year variability in nutrient concentrations and fluxes driven in part by background variability in meteorological and inflow driver data. The use of whole-ecosystem simulation models to detect relatively small changes in nutrient concentrations can provide important insights into how lake nutrient cycling at the ecosystem scale may change over decadal scales. While our focus here was on the GLM-AED ecosystem model, we note that other approaches, including mesocosm experiments, field surveys, and statistical models (reviewed by Jeppesen et al., 2014), also provide valuable context for understanding ecosystem responses to warming. Indeed, a combination of modeling and empirical approaches will likely provide the strongest insights about potential future changes in lake responses to warming.

#### 4.4. Lake warming in the context of climate change

Climate change is expected to elicit non-linear, interconnected

changes in lake ecosystem functions. While our lake models simulate many interconnected ecosystem-scale biogeochemical processes that will change in response to the direct effects of increasing air temperature, our relatively simplistic uniform year-round air temperature scenarios do not account for potential effects of variability in air temperature warming (Hayhoe et al., 2010, 2008), which will affect the onset and intensity of seasonal stratification, and in turn nutrient cycling. In addition, our current approach does not include potential indirect effects of warming and other aspects of climate change that are likely to affect nutrient cycling in Lake Mendota and Lake Sunapee. For example, climate warming is expected to change the timing and intensity of precipitation (e.g., Mearns et al., 2013) and increase upstream nutrient leaching in temperate lake catchments (Jeppesen et al., 2010, 2009), which would affect inflow water volumes and nutrient concentrations for our model lakes. Such changes could be further compounded by human-driven land use change in lake watersheds, resulting in dramatically altered nutrient loading to lakes (Cobourn et al., 2018; Fraterrigo and Downing, 2008). In addition, warming temperatures will alter the phytoplankton community (reviewed by Carey et al., 2012), such that the current model parameterization of phytoplankton functional groups is unlikely to be representative of future communities. Further, it is likely that warming will also alter lake carbon dynamics in addition to nitrogen and phosphorus cycling (Bartosiewicz et al., 2019). Using a coupled catchment-lake model and harnessing the power of the GRAPLEr distributed computing framework (Subratie et al., 2017a) in future work to generate millions of additional scenarios that explore the interactive effects and potential emergent properties of multiple global change variables would greatly improve our understanding of the nuanced ways that climate change will likely affect lakes. In addition, it is possible that different model parameterizations would result in different nutrient responses; however, the similarity of relative changes in water temperature, thermal stratification, denitrification, sediment P fluxes, and summer TN export between the two lakes calibrated to represent varying trophic states suggests that lake results are robust.

Finally, while our analysis focused on the stratified period of Lake Mendota and Lake Sunapee (1 April to 31 October), as north temperate, dimictic lakes, both lakes currently experience ice-covered periods for multiple months each winter (Bruesewitz et al., 2015; Magee et al., 2016). Across the full year, warming may exacerbate changes in nutrient processing and retention in our focal lakes, as increased air temperatures reduce ice-cover duration and ice thickness (e.g., Magee and Wu, 2017b). Despite these limitations, our study provides evidence that ecosystem-scale nutrient concentrations can change, sometimes substantially, due to increases in air temperature alone; thus, decreases in inflow nutrients could help alleviate the expected effects of climate warming.

#### CRediT authorship contribution statement

**Kaitlin J. Farrell:** Conceptualization, Methodology, Data curation, Validation, Formal analysis, Visualization, Writing - original draft. **Nicole K. Ward:** Conceptualization, Data curation, Validation, Visualization, Writing - original draft. **Arianna I. Krinos:** Conceptualization, Methodology, Writing - review & editing. **Paul C. Hanson:** Conceptualization, Methodology, Data curation, Validation, Funding acquisition, Writing - review & editing. **Vahid Daneshmand:** Conceptualization, Software, Writing - review & editing. **Renato J. Figueiredo:** Conceptualization, Software, Resources, Funding acquisition, Writing - review & editing. **Cayelan C. Carey:** Conceptualization, Methodology, Formal analysis, Writing - original draft, Supervision, Funding acquisition.

## Declaration of Competing Interest

None.

## Acknowledgements

This work is part of the Pacific Rim Application and Grid Middleware Assembly (PRAGMA) and Global Lakes Ecological Observatory Network (GLEON) Expedition and leveraged logistical support from the PRAGMA-32 Lake Modeling Workshop (April 2017) in Gainesville, Florida. We thank Grace Hong for facilitating the workshop, and Jon Doubek, Mary Lofton, Ryan McClure, Ken Subratie, Phil Papadopoulos, and Jaikrishna Sukumar for contributing ideas during the workshop. Kathleen Weathers provided valuable feedback on an earlier draft of this manuscript, and Matt Hipsey kindly shared GLM-AED illustrations with us to develop Fig. 2. Data were obtained from the North Temperate Lakes LTER (Mendota) and the Lake Sunapee Protective Association (Sunapee), and we thank Bethel Steele for assistance collating Sunapee data, and acknowledge National Science Foundation (NSF) grant EF 1137327 (K.C. Weathers) for support of Sunapee data collection. This work was supported by NSF grants ACI 1234983, CNS 1737424, DEB 1753639, ICER 1517823, DEB 1926050, and EF 1702506.

## Supplementary materials

Supplementary material associated with this article can be found, in the online version, at [doi:10.1016/j.ecolmodel.2020.109134](https://doi.org/10.1016/j.ecolmodel.2020.109134).

## References

- Abatzoglou, J.T., 2013. Development of gridded surface meteorological data for ecological applications and modelling. *Int. J. Climatol.* 33, 121–131. <https://doi.org/10.1002/joc.3413>.
- Abatzoglou, J.T., Brown, T.J., 2012. A comparison of statistical downscaling methods suited for wildfire applications. *Int. J. Climatol.* 32, 772–780. <https://doi.org/10.1002/joc.2312>.
- Adrian, R., O'Reilly, C.M., Zagarese, H., Baines, S.B., Hessen, D.O., Keller, W., Livingstone, D.M., Sommaruga, R., Straile, D., Van Donk, E., Weyhenmeyer, G.A., Winder, M., 2009. Lakes as sentinels of climate change. *Limnol. Oceanogr.* 54, 2283–2297. [https://doi.org/10.4319/lo.2009.54.6\\_part\\_2.2283](https://doi.org/10.4319/lo.2009.54.6_part_2.2283).
- Arheimer, B., Andréasson, J., Fogelberg, S., Johnsson, H., Pers, C.B., Persson, K., 2005. Climate change impact on water quality: model results from southern Sweden. *Ambio* 34, 559–566. <https://doi.org/10.1579/0044-7447-34.7.559>.
- Arrhenius, S., 1889. Über die Reaktionsgeschwindigkeit bei der Inversion von Rohrzucker durch Säuren. *Zeitschrift für Phys. Chemie* 4, 226–248.
- Bartosiewicz, M., Przytulska, A., Lapiere, J., Laurion, I., Lehmann, M.F., Maranger, R., 2019. Hot tops, cold bottoms: synergistic climate warming and shielding effects increase carbon burial in lakes. *Limnol. Oceanogr. Lett.* 4, 132–144. <https://doi.org/10.1002/lo.2.10117>.
- Beutel, M.W., Horne, A.J., 2018. Nutrient fluxes from profundal sediment of ultra-oligotrophic Lake Tahoe, California/Nevada: implications for water quality and management in a changing climate. *Water Resour. Res.* 54, 1549–1559. <https://doi.org/10.1002/2017WR020907>.
- Bocaniov, S.A., Leon, L.F., Rao, Y.R., Schwab, D.J., Scavia, D., 2016. Simulating the effect of nutrient reduction on hypoxia in a large lake (Lake Erie, USA-Canada) with a three-dimensional lake model. *J. Great Lakes Res.* 42, 1228–1240. <https://doi.org/10.1016/j.jglr.2016.06.001>.
- Bruce, L.C., Frassl, M.A., Arhonditsis, G.B., Gal, G., Hamilton, D.P., Hanson, P.C., Hetherington, A.L., Melack, J.M., Read, J.S., Rinke, K., Rigosi, A., Trolle, D., Winslow, L., Adrian, R., Ayala, A.L., Bocaniov, S.A., Boehrer, B., Boon, C., Brookes, J.D., Bueche, T., Busch, B.D., Copetti, D., Cortés, A., de Eyto, E., Elliott, J.A., Gallina, N., Gilboa, Y., Guynnon, N., Huang, L., Kerimoglu, O., Lenters, J.D., MacIntyre, S., Makler-Pick, V., McBride, C.G., Moreira, S., Özkundakci, D., Piloti, M., Rueda, F.J., Rusak, J.A., Samal, N.R., Schmid, M., Shatwell, T., Snorthheim, C., Soullignac, F., Valerio, G., van der Linden, L., Vetter, M., Vinçon-Leite, B., Wang, J., Weber, M., Wickramaratne, C., Woolway, R.L., Yao, H., Hipsey, M.R., 2018. A multi-lake comparative analysis of the General Lake Model (GLM): stress-testing across a global observatory network. *Environ. Model. Softw.* 102, 274–291. <https://doi.org/10.1016/j.envsoft.2017.11.016>.
- Bruesewitz, D.A., Carey, C.C., Richardson, D.C., Weathers, K.C., 2015. Under-ice thermal stratification dynamics of a large, deep lake revealed by high-frequency data. *Limnol. Oceanogr.* 60, 347–359. <https://doi.org/10.1002/lno.10014>.
- Bueche, T., Hamilton, D.P., Vetter, M., 2017. Using the General Lake Model (GLM) to simulate water temperatures and ice cover of a medium-sized lake: a case study of Lake Ammersee. *Environ. Earth Sci.* 76, 1–14. <https://doi.org/10.1007/s12665-017-6790-7>.
- Bueche, T., Vetter, M., 2015. Future alterations of thermal characteristics in a medium-sized lake simulated by coupling a regional climate model with a lake model. *Clim. Dyn.* 44, 371–384. <https://doi.org/10.1007/s00382-014-2259-5>.
- Burkett, V.R., Wilcox, D.A., Stottlemeyer, R., Barrow, W., Fagre, D., Baron, J., Price, J., Nielsen, J.L., Allen, C.D., Peterson, D.L., Ruggerone, G., Doyle, T., 2005. Nonlinear dynamics in ecosystem response to climatic change: case studies and policy implications. *Ecol. Complex.* 2, 357–394. <https://doi.org/10.1016/J.ECOCOM.2005.04.010>.
- Butcher, J.B., Nover, D., Johnson, T.E., Clark, C.M., 2015. Sensitivity of lake thermal and mixing dynamics to climate change. *Clim. Change* 129, 295–305. <https://doi.org/10.1007/s10584-015-1326-1>.
- Butcher, J.B., Zi, T., Schmidt, M., Johnson, T.E., Nover, D.M., Clark, C.M., 2017. Estimating future temperature maxima in lakes across the United States using a surrogate modeling approach. *PLoS ONE* 12, e0183499. <https://doi.org/10.1371/journal.pone.0183499>.
- Carey, C.C., Ibelings, B.W., Hoffmann, E.P., Hamilton, D.P., Brookes, J.D., 2012. Eco-physiological adaptations that favour freshwater cyanobacteria in a changing climate. *Water Res.* 46, 1394–1407. <https://doi.org/10.1016/j.watres.2011.12.016>.
- Carey, C.C., Weathers, K.C., Ewing, H.A., Greer, M.L., Cottingham, K.L., 2014. Spatial and temporal variability in recruitment of the cyanobacterium *Gloeotrichia echinulata* in an oligotrophic lake. *Freshw. Sci.* 33, 577–592. <https://doi.org/10.1086/675734>.
- Carpenter, S.R. (Ed.), 1988. Complex interactions in lake communities. Springer-Verlag New York. <https://doi.org/10.1007/978-1-4612-3838-6>.
- Cavalcanti, J.R., da Motta-Marques, D., Fragosó, C.R., 2016. Process-based modeling of shallow lake metabolism: spatio-temporal variability and relative importance of individual processes. *Ecol. Modell.* 323, 28–40. <https://doi.org/10.1016/j.ecolmodel.2015.11.010>.
- Cobourn, K.M., Carey, C.C., Boyle, K.J., Duffy, C., Dugan, H.A., Farrell, K.J., Fitchett, L., Hanson, P.C., Hart, J.A., Henson, V.R., Hetherington, A.L., Kemanian, A.R., Rudstam, L.G., Shu, L., Soranno, P.A., Sorice, M.G., Stachelek, J., Ward, N.K., Weathers, K.C., Weng, W., Zhang, Y., 2018. From concept to practice to policy: modeling coupled natural and human systems in lake catchments. *Ecosphere* 9, e02209. <https://doi.org/10.1002/ecs2.2209>.
- Collins, S.M., Yuan, S., Tan, P.N., Oliver, S.K., Lapierre, J.F., Cheruvilil, K.S., Fergus, C.E., Skaff, N.K., Stachelek, J., Wagner, T., Soranno, P.A., 2019. Winter precipitation and summer temperature predict lake water quality at macroscales. *Water Resour. Res.* 55, 2708–2721. <https://doi.org/10.1029/2018WR023088>.
- Fang, X., Alam, S.R., Stefan, H.G., Jiang, L., Jacobson, P.C., Pereira, D.L., 2012. Simulations of water quality and oxythermal crisis habitat in Minnesota lakes under past and future climate scenarios. *Water Qual. Res. J. Canada* 47, 375–388. <https://doi.org/10.2166/wqrj.2012.031>.
- Fenocchi, A., Rogora, M., Sibilla, S., Ciampittello, M., Dresti, C., 2018. Forecasting the evolution in the mixing regime of a deep subalpine lake under climate change scenarios through numerical modelling (Lake Maggiore, Northern Italy/Southern Switzerland). *Clim. Dyn.* 51, 3521–3536. <https://doi.org/10.1007/s00382-018-4094-6>.
- Foley, B., Jones, I.D., Maberly, S.C., Rippey, B., 2012. Long-term changes in oxygen depletion in a small temperate lake: effects of climate change and eutrophication. *Freshw. Biol.* 57, 278–289. <https://doi.org/10.1111/j.1365-2427.2011.02662.x>.
- Fordham, D.A., 2015. Mesocosms reveal ecological surprises from climate change. *PLoS Biol* 13, e1002323. <https://doi.org/10.1371/journal.pbio.1002323>.
- Fraterrigo, J.M., Downing, J.A., 2008. The influence of land use on lake nutrients varies with watershed transport capacity. *Ecosystems* 11, 1021–1034. <https://doi.org/10.1007/s10021-008-9176-6>.
- Gal, G., Hipsey, M.R., Parparov, A., Wagner, U., Makler, V., Zohary, T., 2009. Implementation of ecological modeling as an effective management and investigation tool: lake Kinneret as a case study. *Ecol. Modell.* 220, 1697–1718. <https://doi.org/10.1016/j.ecolmodel.2009.04.010>.
- Gerling, A.B., Munger, Z.W., Doubek, J.P., Hamre, K.D., Gantzer, P.A., Little, J.C., Carey, C.C., 2016. Whole-catchment manipulations of internal and external loading reveal the sensitivity of a century-old reservoir to hypoxia. *Ecosystems* 19, 555–571. <https://doi.org/10.1007/s10021-015-9951-0>.
- Hamilton, D.P., Schladow, S.G., 1997. Prediction of water quality in lakes and reservoirs. Part I - Model description. *Ecol. Modell.* 96, 91–110. [https://doi.org/10.1016/S0304-3800\(96\)00062-2](https://doi.org/10.1016/S0304-3800(96)00062-2).
- Havens, K., Jeppesen, E., 2018. Ecological responses of lakes to climate change. *Water (Switzerland)* 10, 1–9. <https://doi.org/10.3390/w10070917>.
- Hayhoe, K., VanDorn, J., Croley, T., Schlegal, N., Wuebbles, D., 2010. Regional climate change projections for Chicago and the US Great Lakes. *J. Great Lakes Res.* 36, 7–21. <https://doi.org/10.1016/j.jglr.2010.03.012>.
- Hayhoe, K., Wake, C., Anderson, B., Liang, X.-Z., Maurer, E., Zhu, J., Bradbury, J., DeGaetano, A., Stoner, A.M., Wuebbles, D., 2008. Regional climate change projections for the Northeast USA. *Mitig. Adapt. Strateg. Glob. Change* 13, 425–436. <https://doi.org/10.1007/s11027-007-9133-2>.
- Hipsey, M.R., Bruce, L.C., Boon, C., Busch, B., Carey, C.C., Hamilton, D.P., Hanson, P.C., Read, J.S., De Sousa, E., Weber, M., Winslow, L.A., 2019. A General Lake Model (GLM 3.0) for linking with high-frequency sensor data from the Global Lake Ecological Observatory Network (GLEON). *Geosci. Model Dev.* 12, 473–523. <https://doi.org/10.5194/gmd-12-473-2019>.
- Hipsey, M.R., Bruce, L.C., Hamilton, D.P., 2014. AED Report #26. The University of Western Australia, Perth, Australia, pp. 42.
- Hipsey, M.R., Bruce, L.C., Hamilton, D.P., 2013. Aquatic Ecodynamics (AED) Model Library Science Manual, October 2013. Available: [http://aed.see.uwa.edu.au/research/models/aed/Download/AED\\_ScienceManual\\_v4\\_draft.pdf](http://aed.see.uwa.edu.au/research/models/aed/Download/AED_ScienceManual_v4_draft.pdf).
- Ito, Y., Momii, K., 2015. Impacts of regional warming on long-term hypolimnetic anoxia

- and dissolved oxygen concentration in a deep lake. *Hydrol. Process.* 29, 2232–2242. <https://doi.org/10.1002/hyp.10362>.
- Jeppesen, E., Kronvang, B., Meerhoff, M., Søndergaard, M., Hansen, K.M., Andersen, H.E., Lauridsen, T.L., Liboriussen, L., Beklioglu, M., Ozen, A., Olesen, J.E., Ozen, A., Olesen, J.E., 2009. Climate change effects on runoff, catchment phosphorus loading and lake ecological state, and potential adaptations. *J. Environ. Qual.* 38, 1930–1941. <https://doi.org/10.2134/jeq2008.0113>.
- Jeppesen, E., Meerhoff, M., Davidson, T.A., Trolle, D., Søndergaard, M., Lauridsen, T.L., Beklioglu, M., Brucet, S., Volta, P., González-Bergonzoni, I., Nielsen, A., 2014. Climate change impacts on lakes: an integrated ecological perspective based on a multi-faceted approach, with special focus on shallow lakes. *J. Limnol.* 73, 88–111. <https://doi.org/10.4081/jlimnol.2014.844>.
- Jeppesen, E., Olesen, J.E., Ozen, A., Larsen, S.E., Kronvang, B., Meerhoff, M., Liboriussen, L., Andersen, H.E., Lauridsen, T.L., Özkán, K., Hoffmann, C.C., Søndergaard, M., Audet, J., Beklioglu, M., 2010. Climate change effects on nitrogen loading from cultivated catchments in Europe: implications for nitrogen retention, ecological state of lakes and adaptation. *Hydrobiologia* 663, 1–21. <https://doi.org/10.1007/s10750-010-0547-6>.
- Jiménez Cisneros, B.E., Oki, T., Arnell, N.W., Benito, G., Cogley, J.G., Döll, P., Jiang, T., Mwakalila, S.S., 2014. Freshwater resources. In: Field, C.B., Barros, V.R., Dokken, D.J., Mach, K.J., Mastrandrea, M.D., Bilir, T.E. (Eds.), *Climate Change 2014: Impacts, Adaptation, and Vulnerability. Part A: Global and Sectoral Aspects. Contribution of Working Group II to the Fifth Assessment Report of the Intergovernmental Panel On Climate Change*. Cambridge University Press, Cambridge, United Kingdom, pp. 229–269 and New York, NY.
- Kara, E.L., Hanson, P.C., Hamilton, D.P., Hipsey, M.R., McMahon, K.D., Read, J.S., Winslow, L.A., Dedrick, J., Rose, K., Carey, C.C., Bertilsson, S., da Motta Marques, D., Beversdorf, L., Miller, T., Wu, C., Hsieh, Y.F., Gaiser, E., Kratz, T., 2012. Time-scale dependence in numerical simulations: assessment of physical, chemical, and biological predictions in a stratified lake at temporal scales of hours to months. *Environ. Model. Softw.* 35, 104–121. <https://doi.org/10.1016/j.envsoft.2012.02.014>.
- Kelly, P., Renwick, W.H., Knoll, L., Vanni, M., 2019. Stream nitrogen and phosphorus loads are differentially affected by storm events, and the difference may be exacerbated by conservation tillage. *Environ. Sci. Technol.* 5613–5621. <https://doi.org/10.1021/acs.est.8b05152>.
- Komatsu, E., Fukushima, T., Harasawa, H., 2007. A modeling approach to forecast the effect of long-term climate change on lake water quality. *Ecol. Modell.* 209, 351–366. <https://doi.org/10.1016/j.ecolmodel.2007.07.021>.
- Kraemer, B., Anneville, O., Chandra, S., Dix, M., Kuusisto, E., Livingstone, D.M., Rimmer, A., Schladow, S.G., Silow, E., Sitoki, L.M., Tamatamah, R., Vadeboncoeur, Y., McIntyre, P.B., 2015. Morphometry and average temperature affect stratification responses to climate change. *Geophys. Res. Lett.* 42, 4981–4988. <https://doi.org/10.1002/2015GL064097>.
- Lathrop, R.C., Carpenter, S.R., 2014. Water quality implications from three decades of phosphorus loads and trophic dynamics in the Yahara chain of lakes. *Int. Waters* 4, 1–14. <https://doi.org/10.5268/IW-4.1.680>.
- Lewis Jr., W.M., 2002. Causes for the high frequency of nitrogen limitation in tropical lakes. *Verhandlungen des Int. Verein Limnol.* 28, 210–213. <https://doi.org/10.1080/03680770.2001.11902574>.
- Lewis Jr., W.M., 1996. Tropical lakes: how latitude makes a difference. In: Schiemer, F., Boland, K.T. (Eds.), *Perspectives in Tropical Limnology*. SPB Academic Publishing, Amsterdam, pp. 43–64.
- Magee, M.R., McIntyre, P.B., Hanson, P.C., Wu, C.H., 2019. Drivers and management implications of long-term cisco oxythermal habitat decline in Lake Mendota. *WI. Environ. Manage.* 63, 396–407. <https://doi.org/10.1007/s00267-018-01134-7>.
- Magee, M.R., Wu, C.H., 2017a. Response of water temperatures and stratification to changing climate in three lakes with different morphometry. *Hydrol. Earth Syst. Sci.* 21, 6253–6274. <https://doi.org/10.5194/hess-21-6253-2017>.
- Magee, M.R., Wu, C.H., 2017b. Effects of changing climate on ice cover in three morphometrically different lakes. *Hydrol. Process.* 31, 308–323. <https://doi.org/10.1002/hyp.10996>.
- Magee, M.R., Wu, C.H., Robertson, D.M., Lathrop, R.C., Hamilton, D.P., 2016. Trends and abrupt changes in 104 years of ice cover and water temperature in a dimictic lake in response to air temperature, wind speed, and water clarity drivers. *Hydrol. Earth Syst. Sci.* 20, 1681–1702. <https://doi.org/10.5194/hess-20-1681-2016>.
- Magnuson, J., Carpenter, S.R., Stanley, E.H., 2010a. North Temperate Lakes LTER: chemical limnology of primary study lakes: nutrients, pH and carbon 1981-current. *Environ. Data Initiat.* <https://doi.org/10.6073/pasta/88bf494f2f8042cb18e3ee81a9751b98>.
- Magnuson, J., Carpenter, S.R., Stanley, E.H., 2010b. North Temperate Lakes LTER: high frequency data: meteorological, dissolved oxygen, chlorophyll, phycocyanin- Lake Mendota buoy 2006-current. *Environ. Data Initiat.* <https://doi.org/10.6073/pasta/9bced2f6ff81aa30f0f573766c0a410b>.
- Magnuson, J., Carpenter, S.R., Stanley, E.H., 2010c. North Temperate Lakes LTER: high frequency water temperature data- Lake Mendota buoy 2006-current. *Environ. Data Initiat.* <https://doi.org/10.6073/pasta/e15bf301e7ddbfaebfdee873a2b4c19>.
- Magnuson, J., Carpenter, S.R., Stanley, E.H., 2010d. North Temperate Lakes LTER: physical limnology of primary study lakes 1981-current. *Environ. Data Initiat.* <https://doi.org/10.6073/pasta/b6b592b542c91909a81272ff8d92a6c6>.
- Malmäus, J.M., Blenckner, T., Markensten, H., Persson, I., 2006. Lake phosphorus dynamics and climate warming: a mechanistic model approach. *Ecol. Modell.* 190, 1–14. <https://doi.org/10.1016/j.ecolmodel.2005.03.017>.
- Marcé, R., Rodríguez-Arias, M.A., García, J.C., Armengol, J.O.A.N., 2010. El Niño southern oscillation and climate trends impact reservoir water quality. *Glob. Chang. Biol.* 16, 2857–2865. <https://doi.org/10.1111/j.1365-2486.2010.02163.x>.
- Mearns, L.O., Sain, S., Leung, L.R., Bukovsky, M.S., McGinnis, S., Biner, S., Caya, D., Arritt, R.W., Gutowski, W., Takle, E., 2013. Climate change projections of the North American regional climate change assessment program (NARCCAP). *Clim. Change* 120, 965–975. <https://doi.org/10.1007/s10584-013-0831-3>.
- Moss, B., 2012. Cogs in the endless machine: lakes, climate change and nutrient cycles: a review. *Sci. Total Environ.* 434, 130–142. <https://doi.org/10.1016/j.scitotenv.2011.07.069>.
- North, R.P., North, R.L., Livingstone, D.M., Köster, O., Kipfer, R., 2014. Long-term changes in hypoxia and soluble reactive phosphorus in the hypolimnion of a large temperate lake: consequences of a climate regime shift. *Glob. Chang. Biol.* 20, 811–823. <https://doi.org/10.1111/gcb.12371>.
- Nürnberg, G.K., 1984. The prediction of internal phosphorus load in lakes with anoxic hypolimnia. *Limnol. Oceanogr.* 29, 111–124. <https://doi.org/10.4319/lo.1984.29.1.0111>.
- O'Reilly, C.M., Rowley, R.J., Schneider, P., Lenters, J.D., McIntyre, P.B., Kraemer, B.M., 2015. Rapid and highly variable warming of lake surface waters around the globe. *Geophys. Res. Lett.* 42 (10) 773–10,781. <https://doi.org/10.1002/2015GL066235>.
- Palmer, M.E., Yan, N.D., Somers, K.M., 2014. Climate change drives coherent trends in physics and oxygen content in North American lakes. *Clim. Change* 124, 285–299. <https://doi.org/10.1007/s10584-014-1085-4>.
- Parrott, L., Meyer, W.S., 2012. Future landscapes: managing within complexity. *Front. Ecol. Environ.* 10, 382–389. <https://doi.org/10.1890/110082>.
- Pettersson, K., Grust, K., Weyhenmeyer, G., Blenckner, T., 2003. Seasonality of chlorophyll and nutrients in Lake Erken - Effects of weather conditions. *Hydrobiologia* 506–509, 75–81. <https://doi.org/10.1023/B:HYDR.0000008582.61851.76>.
- Powers, S.M., Tank, J.L., Robertson, D.M., 2015. Control of nitrogen and phosphorus transport by reservoirs in agricultural landscapes. *Biogeochemistry* 124, 417–439. <https://doi.org/10.1007/s10533-015-0106-3>.
- Prein, A.F., Rasmussen, R.M., Ikeda, K., Liu, C., Clark, M.P., Holland, G.J., 2017. The future intensification of hourly precipitation extremes. *Nat. Clim. Chang.* 7, 48–52. <https://doi.org/10.1038/nclimate3168>.
- R. Core Team, 2019. R: a language and environment for statistical computing.
- Radbourne, A.D., Elliott, J.A., Maberly, S.C., Ryves, D.B., Anderson, N.J., 2019. The impacts of changing nutrient load and climate on a deep, eutrophic, monomictic lake. *Freshw. Biol.* 64, 1169–1182. <https://doi.org/10.1111/fwb.13293>.
- Razali, N.M., Wah, Y.B., 2011. Power comparisons of Shapiro-Wilk, Kolmogorov-Smirnov, Lilliefors and Anderson-Darling tests. *J. Stat. Model. Anal.* 2, 21–33. <https://doi.org/10.1515/bile-2015-0008>.
- Read, J., Hamilton, D., Jones, I., Muraoka, K., Winslow, L., Kroiss, R., Wu, C., Gaiser, E., 2011. Derivation of lake mixing and stratification indices from high-resolution lake buoy data. *Environ. Model. Softw.* 26, 1325–1336. <https://doi.org/10.1016/j.envsoft.2011.05.006>.
- Reynolds, C.S., 2006. *The ecology of phytoplankton*. Cambridge University Press, Cambridge, United Kingdom.
- Richardson, D.C., Carey, C.C., Bruesewitz, D.A., Weathers, K.C., 2017a. Intra- and inter-annual variability in metabolism in an oligotrophic lake. *Aquat. Sci.* 79, 319–333. <https://doi.org/10.1007/s00027-016-0499-7>.
- Richardson, D.C., Carey, C.C., Weathers, K.C., Bruesewitz, D.A., LSPA, L.S.P.A., Steele, B.G., 2020. High frequency meteorological, drift-corrected dissolved oxygen, and thermistor temperature data - Lake Sunapee Buoy, NH, USA, 2007 – 2013. *Environ. Data Initiat.* <https://doi.org/10.6073/pasta/846a36bf6fd704e508511e5f8a2ab3b5>.
- Richardson, D.C., Melles, S.J., Pilla, R.M., Hetherington, A.L., Knoll, L.B., Williamson, C.E., Kraemer, B.M., Jackson, J.R., Long, E.C., Moore, K., Rudstam, L.G., Rusak, J.A., Saros, J.E., Sharma, S., Strock, K.E., Weathers, K.C., Wigdahl-Perry, C.R., 2017b. Transparency, geomorphology and mixing regime explain variability in trends in lake temperature and stratification across Northeastern North America (1975–2014). *Water* 9, 442. <https://doi.org/10.3390/w9060442>.
- Sahoo, G.B., Schladow, S.G., Reuter, J.E., Coats, R., Dettinger, M., Riverson, J., Wolfe, B., Costa-Cabral, M., 2013. The response of Lake Tahoe to climate change. *Clim. Change* 116, 71–95. <https://doi.org/10.1007/s10584-012-0600-8>.
- Shaver, G.R., Canadell, J., Chapin, F.S., Gurevitch, J., Harte, J., Henry, G., Ineson, P., Jonasson, S., Melillo, J., Pitelka, L., Rustad, L., 2000. Global warming and terrestrial ecosystems: a conceptual framework for analysis. *Bioscience* 50, 871. [https://doi.org/10.1641/0006-3568\(2000\)050\[0871:gwatae\]2.0.co;2](https://doi.org/10.1641/0006-3568(2000)050[0871:gwatae]2.0.co;2).
- Snorheim, C.A., Hanson, P.C., McMahon, K.D., Read, J.S., Carey, C.C., Dugan, H.A., 2017. Meteorological drivers of hypolimnetic anoxia in a eutrophic, north temperate lake. *Ecol. Modell.* 343, 39–53. <https://doi.org/10.1016/j.ecolmodel.2016.10.014>.
- Solomon, C.T., Bruesewitz, D.A., Richardson, D.C., Rose, K.C., Van de Bogert, M.C., Hanson, P.C., Kratz, T.K., Larget, B., Adrian, R., Babin, B.L., Chiu, C.Y., Hamilton, D.P., Gaiser, E.E., Hendricks, S., Istvanovics, V., Laas, A., O'Donnell, D.M., Pace, M.L., Ryder, E., Staehr, P.A., Torgersen, T., Vanni, M.J., Weathers, K.C., Zhu, G., Leroux Babin, B., Chiu, C.Y., Hamilton, D.P., Gaiser, E.E., Hendricks, S., Istvá, V., Laas, A., O'Donnell, D.M., Pace, M.L., Ryder, E., Staehr, P.A., Torgersen, T., Vanni, M.J., Weathers, K.C., Zhu, G., 2013. Ecosystem respiration: drivers of daily variability and background respiration in lakes around the globe. *Limnol. Oceanogr.* 58, 849–866. <https://doi.org/10.4319/lo.2013.58.3.0849>.
- Stefan, H.G., Hondzo, M., Fang, X., 1993. Lake water quality modeling for projected future climate scenarios. *J. Environ. Qual.* 22, 417–431. <https://doi.org/10.2134/jeq1993.00472425002200030005x>.
- Steiner, S., Titus, M., 2017. NH Department of Environmental Services (NHDES) Watershed Management Bureau Biology Section: volunteer Lake Assessment Program (VLAP) Environmental Monitoring data. *Environ. Data Initiat.* 1995–2014. <https://doi.org/10.6073/pasta/1df3238af71108db248f667b9561023d>.
- Stoddard, J.L., Van Sickle, J., Herlihy, A.T., Brahm, J., Paulsen, S., Peck, D.V., Mitchell, R., Pollard, A.I., 2016. Continental-scale increase in lake and stream phosphorus: are oligotrophic systems disappearing in the United States? *Environ. Sci. Technol.* 50, 3409–3415. <https://doi.org/10.1021/acs.est.5b05950>.

- Stumm, W., Morgan, J.J., 1996. *Aquatic Chemistry: Chemical Equilibria and Rates in Natural Waters*, 3rd ed. John Wiley & Sons, Inc., New York, NY.
- Subratie, K., Aditya, S., Mahesula, S., Figueiredo, R., Carey, C.C., Hanson, P.C., 2017a. GRAPLE: a distributed collaborative environment for lake ecosystem modeling that integrates overlay networks, high-throughput computing, and WEB services. *Concurr. Comput. Pract. Exp.* 29, e4139. <https://doi.org/10.1002/cpe.4139>.
- Subratie, K., Aditya, S., Sabogal, S., Theegala, T., Figueiredo, R.J., 2017b. Towards dynamic, isolated work-groups for distributed IoT and cloud systems with peer-to-peer virtual private networks. In: *Sensors to Cloud Architectures Workshop (SCAW-2017)*. Austin, TX, USA.
- Talling, J.F., Lemoalle, J., 1998. *Ecological Dynamics of Tropical Inland Waters*. Cambridge University Press, Cambridge, United Kingdom.
- Taylor, K.E., Stouffer, R.J., Meehl, G.A., 2012. An overview of CMIP5 and the experiment design. *Bull. Am. Meteorol. Soc.* 93, 485–498 <https://doi.org/10.1175/BAMS-Ddd-11-00094.1>.
- Wetzel, R.G., 2001. *Limnology*, 3rd ed. Elsevier, San Diego, CA.
- Wilhelm, S., Adrian, R., 2008. Impact of summer warming on the thermal characteristics of a polymictic lake and consequences for oxygen, nutrients and phytoplankton. *Freshw. Biol.* 53, 226–237. <https://doi.org/10.1111/j.1365-2427.2007.01887.x>.
- Winder, M., Reuter, J.E., Schladow, S.G., 2009. Lake warming favours small-sized planktonic diatom species. *Proc. R. Soc. B Biol. Sci.* 276, 427–435. <https://doi.org/10.1098/rspb.2008.1200>.
- Woolway, R.I., Maberly, S.C., Jones, I.D., Feuchtmayr, H., 2014. A novel method for estimating the onset of thermal stratification in lakes from surface water measurements. *Water Resour. Res.* 50, 5131–5140. <https://doi.org/10.1002/2013WR014975>.
- Woolway, R.I., Merchant, C.J., 2019. Worldwide alteration of lake mixing regimes in response to climate change. *Nat. Geosci.* 12, 271–276. <https://doi.org/10.1038/s41561-019-0322-x>.
- Zambrano-Bigiarini, M., 2017. hydroGOF: goodness-of-fit functions for comparison of simulated and observed hydrological time series. R Packag. version 0.3–10. <https://doi.org/10.5281/zenodo.840087>.